REPORT DOCUMENTATION PAGE

Form Approved OMB NO. 0704-0188

1. AGENCY USE ONLY (Leave Blank)	2. REPORT DATE:	3. REPORT TYPE AND DATES COVERED
		Final Report 1-Jun-2002 - 30-Nov-2005

4. TITLE AND SUBTITLE	5. FUNDING NUMBERS
Raman-Controlled Quantum Dots for Quantum Computing	DAAD190210183

6. AUTHORS	8. PERFORMING ORGANIZATION REPORT NUMBER
Lu J. Sham	

7. PERFORMING ORGANIZATION NAMES AND ADDRESSES	
University of California - San Diego Office of Contract & Grant Administration 9500 Gilman Drive, Mail Code 0934 La Jolla, CA 92093 -0934	

9. SPONSORING/MONITORING AGENCY NAME(S) AND ADDRESS(ES)	10. SPONSORING / MONITORING AGENCY REPORT NUMBER
U.S. Army Research Office P.O. Box 12211 Research Triangle Park, NC 27709-2211	44058-PH-QC.1

11. SUPPLEMENTARY NOTES

12. DISTRIBUTION AVAILIBILITY STATEMENT	12b. DISTRIBUTION CODE
Approved for Public Release; Distribution Unlimited	

13. ABSTRACT (Maximum 200 words)

The abstract is below since many authors do not follow the 200 word limit

14. SUBJECT TERMS		15. NUMBER OF PAGES
Quantum computing, semiconductor quantum dots, coherent optics, quantum information, optical control		Unknown due to possible attachments
		16. PRICE CODE

17. SECURITY CLASSIFICATION OF REPORT	18. SECURITY CLASSIFICATION ON THIS PAGE	19. SECURITY CLASSIFICATION OF ABSTRACT	20. LIMITATION OF ABSTRACT
UNCLASSIFIED	UNCLASSIFIED	UNCLASSIFIED	UL

NSN 7540-01-280-5500

Standard Form 298 (Rev .2-89)
Prescribed by ANSI Std.
239-18 298-102

Report Title

Optically Controlled Quantum Dots for Quantum Computing

ABSTRACT

Optical control is fundamental to our project objective of demonstration of key quantum operations for quantum computation with spin qubits of electrons in semiconductor quantum dots. Sophia Economou, the graduate student supported by this fellowship, works on the design of optical control taking into account the deterioration of the quantum states of the electron spin and of the excited state during the optical control process. She has three major accomplishments: (1) She and collaborators predicted how spontaneously generated spin coherence by optical excitation affects the spin precession, which was experimentally confirmed. (2) She and collaborators constructed a unified theory of the quantum dynamics of any three level system under a wide range of control and measurement scenarios and under environmental influence, applicable to solid state and atomic systems. (3) She designed and simulated a simple sequence of three pulses to initialize, rotate and inverse-rotate an electron spin qubit. Experimental demonstration has been carried out by our collaborators, D. G. Steel and Yanwen Wu, also under the ARO auspice. She has also helped analyze the data. Both theory and experiment will be presented at CLEO in May 2006. Economou is writing her Ph.D. thesis.

List of papers submitted or published that acknowledge ARO support during this reporting period. List the papers, including journal references, in the following categories:

(a) Papers published in peer-reviewed journals (N/A for none)

1. Sophia E. Economou, Ren-Bao Liu, L. J. Sham, and D. G. Steel, "Unified theory of consequences of spontaneous emission in a system", Phys. Rev. B, 71, 195327 (2005), 11 pages.
2. M.V. Gurudev Dutt, Jun Cheng, Bo Li, Xiaodong Xu, Xiaoqin Li, P. R. Berman, D. G. Steel, A. S. Bracker, D. Gammon, Sophia E. Economou, Ren-Bao Liu, and L. J. Sham, "Stimulated and Spontaneous Optical Generation of Electron Spin Coherence in Charged GaAs Quantum Dots", Phys. Rev. Lett., 94, 227403 (2005), 4 pages.

Number of Papers published in peer-reviewed journals: 2.00

(b) Papers published in non-peer-reviewed journals or in conference proceedings (N/A for none)

1. Sophia E. Economou, Ren-Bao Liu, and L. J. Sham, "Theory of spontaneously generated spin coherence in nanodots", CLEO/QELS 2005, Optical Society of America, May, 2005.
2. Sophia Economou, L. J. Sham, Yanwen Wu, and D. G. Steel, "Theory proposal of electron spin rotation in a quantum dot", CLEO/QELS 2006, Optical Society of America, May, 2006. Accepted for oral presentation and publication.
3. Yanwen Wu, Erik D. Kim, Jun Cheng, Xiaodong Xu, Qiong Huang, Hailing Cheng, and D. G. Steel, Sophia Economou, and L. J. Sham, "Coherent ultrafast optically controlled rotation of electron spins in charged quantum dots", CLEO/QELS 2006, Optical Society of America, May, 2006. Accepted for oral presentation and publication.

Number of Papers published in non peer-reviewed journals: 3.00

(c) Papers presented at meetings, but not published in conference proceedings (N/A for none)

Number of Papers not Published: 0.00

(d) Manuscripts

Number of Manuscripts: 0.00

Number of Inventions:

Graduate Students

NAME	PERCENT_SUPPORTED	
Sophia Economou	1.00	No
FTE Equivalent:	**1.00**	
Total Number:	**1**	

Names of Post Doctorates

NAME	PERCENT_SUPPORTED
FTE Equivalent:	
Total Number:	

Names of Faculty Supported

NAME	PERCENT_SUPPORTED
FTE Equivalent:	
Total Number:	

Names of Under Graduate students supported

NAME	PERCENT_SUPPORTED
FTE Equivalent:	
Total Number:	

Names of Personnel receiving masters degrees

NAME
Total Number:

Names of personnel receiving PHDs

NAME
Total Number:

Names of other research staff

NAME	PERCENT_SUPPORTED
FTE Equivalent:	
Total Number:	

Sub Contractors (DD882)

Inventions (DD882)

I. SCIENTIFIC PROGRESS AND ACCOMPLISHMENT

Problem

Ms Sophia Economou is the graduate student supported by this fellowship to carry out a study of the theory of using coherent light to control the spin-dependent optical transitions of the electrons in dots as a physical basis for the implementation of quantum operations on the spin qubits, basic to quantum computation and information processing. This is in support of the collaboration among three teams at NRL (leader Dan Gammon), Michigan (leader Duncan G. Steel) and UCSD (Lu J. Sham) in experimental demonstration of the fundamentals of quantum computing.

Significance of her accomplishements

She accomplished the goal of a scheme of initializing a spin qubit with about 50-50 chance and its rotation about the optical axis. The scheme is of sufficient experimental simplicity for demonstration. She has also, through her analysis of the decoherence effects, predicted how the spontaneously generated coherence (previously proposed) affected the electron spin rotations, an effect of great consequence in implementation of quantum control.

Details of the scientific progress

Ms Economou first made a microscopic derivation of a Liouville equation for the optical control of the two-state electron spin in a quantum dot excited to the trion state to include the effects of decoherence. In the process, she found the effects of spontaneously generated coherence on the Raman induced electron spin coherence which could be measured [Conference publication 1]. The predicted changes as a function of magnetic field in phase and amplitude of the spin precession were indeed found experimentally [Journal publication 2]. In collaboration with Liu and Sham, Economou built a complete theoretical framework to understand the differences and similarities of different physical systems, such as atoms, ions and quantum dots, in their Raman process behavior. The driving principle identified is the interplay between the symmetry breaking due to external fields and the selection rules of optical transitions. A variety of results follow different measurement paths of the emitted photons in the Raman processes. An exhaustive investigation of the unified theory was published [Journal publication 1].

Ms Economou collaborated with Professor Steel's experimental group by investigating the simplest possible way to demonstrate initialization and a single qubit rotation [Conference publication 2]. Consideration of the dynamics of the spin vector which can be optically excited to the trion states shows the capability of a single pulse to initialize a spin qubit with an ideal efficiency of 50% and the use of a detuned transitionless pulse for a Rabi rotation between one spin state and the trion to effect a $\pi/4$ rotation about the optical axis (z). A static magnetic field in an in-plane direction (x) causes the spin vector to precess in the y-z plane whose projection along the z direction can be optically measured by a probe beam by our experimental group. She has demonstrated by simulation of controlled Raman processes that a single pulse causes a spin qubit initialization close to 50% efficiency, that a subsequent detuned pulse generates a spin rotation from the spin vector when in the -y direction, and that a third one restoring the spin to the spin

state in the -y direction. The optical measurements along of the spin vector along the z direction will show spin oscillations (as have already been experimentally demonstrated) between the first (initialization) pulse and the second (rotation) pulse, and spin oscillations between the second and the third (inverse rotation) pulse. The middle precession train will have a distinctly reduced amplitude because of higher latitude towards the x axis after the $\pi/4$ rotation. The fidelity of the rotation in comparison with the ideal design is calculated in the simulation to be 96%.

Experimental study led by Ms Yanwen Wu [Conference publication 3] showed the generation of spin coherence by the first pulse and phase change effects of a second (control) pulse as functions of the probe time, the time of the control pulse and its pulse area. The phase and amplitude changes after the control pulse can be understood. We are trying to analyze the effects of the imperfect optical Rabi rotation in the second control pulse.

Economou plans to complete her Ph.D. thesis by early May, 2006 and to defend her thesis before the end of May.

II. ATTACHMENT OF 2 PAPERS AND 3 CONFERENCE PROCEEDINGS

Unified theory of consequences of spontaneous emission in a Λ system

Sophia E. Economou,[1] Ren-Bao Liu,[1] L. J. Sham,[1] and D. G. Steel[2]

[1]*Department of Physics, University of California San Diego, La Jolla, California 92093-0319, USA*
[2]*The H. M. Randall Laboratory of Physics, University of Michigan, Ann Arbor, Michigan 48109, USA*

In a Λ system with two nearly degenerate ground states and one excited state in an atom or quantum dot, spontaneous radiative decay can lead to a range of phenomena, including electron-photon entanglement, spontaneously generated coherence, and two-pathway decay. We show that a treatment of the radiative decay as a quantum evolution of a single physical system composed of a three-level electron subsystem and photons leads to a range of consequences depending on the electron-photon interaction and the measurement. Different treatments of the emitted photon channel the electron-photon system into a variety of final states. The theory is not restricted to the three-level system.

I. INTRODUCTION

The electromagnetic vacuum is commonly considered as a reservoir which causes decoherence and decay of a quantum mechanical system coupled to it. An alternative view holds that the two subparts ("quantum system" and "bath") are constituents of a single closed quantum mechanical whole, which is governed by unitary evolution until a projection (measurement) is performed. Different projections may give rise to a variety of phenomena which on the surface appear unrelated. Spontaneous emission is a quantum phenomenon which has been treated in both ways. Its effects are of interest from the views of both fundamental physics and applications.

The radiative decay of a three-level system is attractive for its simplicity and yet richness in physical phenomena. A variety of effects follow from the spontaneous decay. Those which involve semiclassical light and ensemble of atoms include the electromagnetically induced transparency[1] and lasing without inversion.[2] By definition, a Λ system has two nearly degenerate ground states which are dipole coupled to one excited state for optical transitions. We shall, for conciseness, refer to the states as electronic states in an atom or quantum dot. The decoherence and decay effects for a single Λ system are relevant to quantum computing and information processing, for example, in many implementation schemes,[3–7] which can be more practical than the direct excitation of the two-level system.

A Λ system initially in the excited state will eventually decay by the emission of a photon. This process may result in the entanglement of the Λ system with the emitted photon. Recently, entanglement between the hyperfine levels of a trapped ion and the polarization of a photon spontaneously emitted from the ion was demonstrated experimentally.[8]

In quantum optics of the atom, coupling to the modes of the electromagnetic vacuum can contribute to coherence between atomic states, and such terms have been implicit in the textbook treatment of spontaneous radiative decay[9] or indeed explicit in research papers.[10] In the early 1990s, it was pointed out that in a Λ system the spontaneous decay of the highest state to the two lower ones may result in a coherent superposition of the two lower states.[11] The conditions for this spontaneously generated coherence (SGC) as presented in Ref. 11 are that the dipole matrix elements of the two transitions are nonorthogonal and that the difference between the two frequencies is small compared to the radiative linewidth of the excited state.

The final example is the so-called two-pathway decay in which a Λ system—as opposed to a V system—cannot exhibit quantum beats because the information on which the decay path of the system is in principle available by detection of the atom, and therefore no beats are expected (p. 19 of Ref. 12).

All of the phenomena listed above, when viewed separately, appear unrelated, if not down-right contradictory. In fact, they stem from the same process, namely the radiative spontaneous decay of a Λ system. The primary purpose of this paper is to show how they naturally emerge from the same time-evolved composite state of the whole system (Λ subsystem and the electromagnetic modes). From this treatment, follow the conditions for each effect in terms of the electron-photon coupling and in terms of different ways of projecting the photon state by measurement. We also show how a change of symmetry of the system—by the introduction of a perturbation—may determine whether or not a SGC will occur.

The second goal of this work is to analyze these effects in the solid state, where the two lower levels of the Λ system are the spin states of an electron confined in a semiconductor quantum dot. For this system, SGC has been given a theoretical analysis and experimental demonstration,[13] and we further propose here an experiment for the demonstration of spin-photon polarization entanglement. In our treatment, we distinguish between a single system and an ensemble for the various phenomena; in this context, we make a comparative study of the solid-state and the atomic system.

This paper is organized as follows In Sec. II, we present the time evolution of the decay process which leads to the conditions for the occurrence of each of the listed phenomena. In Sec. III, we deduce a set of conditions on the symmetry of the system for SGC. Sections IV and V illustrate these conditions by specific examples from atomic and solid-state systems, respectively. We also present the theory of the

pump-probe experiment and derive the probe signal, which is altered by the SGC term (Sec. VI).

II. SPONTANEOUS EMISSION AS QUANTUM EVOLUTION

Consider a single Λ system in a photon bath with modes $|k\rangle$, where $k=(\mathbf{k},\sigma)$, $\mathbf{k}$ being the wave vector and σ the state with the polarization vector $\boldsymbol{\varepsilon}_\sigma$. In the dipole and rotating-wave approximation, the Hamiltonian for the whole system is given by

$$H = \sum_k \omega_k b_k^\dagger b_k + \sum_{i=1}^{3} \epsilon_i |i\rangle\langle i| + \sum_{k;i=1,2} g_{ik} b_k^\dagger |i\rangle\langle 3|$$
$$+ \sum_{k;i=1,2} g_{ik}^* b_k |3\rangle\langle i|, \qquad (1)$$

where b_k destroys a photon of energy or frequency ω_k ($\hbar=1$) and $|i\rangle$ is the electronic state with energy or frequency ϵ_i. The coupling between the photon and the electron is $g_{ik} \propto \boldsymbol{\varepsilon}_\sigma \cdot \mathbf{d}_i$, where $\mathbf{d}_i$ is the dipole matrix element for the transition $3 \leftrightarrow i$. The Λ system is taken to be at $t=0$ in the excited level $|3\rangle$ (which can be prepared by a short pulse), and the photon bath is in the vacuum state, i.e., the whole system is in a product state. For $t>0$, the composite wave packet can be written as

$$|\psi(t)\rangle \equiv c_3(t)|3\rangle|\mathrm{vac}\rangle + \sum_k c_{1k}(t)|1\rangle|k\rangle + \sum_k c_{2k}(t)|2\rangle|k\rangle,$$
$$(2)$$

where $|\mathrm{vac}\rangle$ is the photon vacuum state. Evolution of this state is governed by the Schrödinger equation.

By the Weisskopf–Wigner theory[14] of spontaneous emission,[12] the coefficient c_3 is obtained by one iteration of the other coefficients:

$$\partial_t c_3 = -i\epsilon_3 c_3 - \sum_k |g_{1k}|^2 \int_0^t e^{-i(\epsilon_1+\omega_k)(t-t')} c_3(t')dt',$$
$$- \sum_k |g_{2k}|^2 \int_0^t e^{-i(\epsilon_2+\omega_k)(t-t')} c_3(t')dt'. \qquad (3)$$

Since the electron–photon coupling is much weaker than the transition energy in the Λ system, the integrals in the equation above can be evaluated in the Markovian approximation, resulting in:

$$\partial_t c_3 \approx -i\epsilon_3 c_3 - \frac{\Gamma_{31}}{2} c_3 - \frac{\Gamma_{32}}{2} c_3, \qquad (4)$$

where

$$\Gamma_{3i} = 2\sum_k |g_{2k}|^2 \int_0^t e^{-i(\epsilon_i+\omega_k)(t-t')} dt'. \qquad (5)$$

Thus, the solution is

$$c_3 \approx e^{-(i\epsilon_3+\Gamma/2)t}, \qquad (6)$$

where $\Gamma \equiv \Gamma_{31}+\Gamma_{32}$ is the radiative linewidth of the excited state. Furthermore, c_{1k} and c_{2k} are given by

$$c_{1k} \approx -\frac{g_{1k}}{\epsilon_3 - \epsilon_1 - \omega_k - i\frac{\Gamma}{2}} \left[e^{-i(\epsilon_1+\omega_k)t} - e^{-i\epsilon_3 t - \frac{\Gamma}{2}t} \right],$$

$$c_{2k} \approx -\frac{g_{2k}}{\epsilon_3 - \epsilon_2 - \omega_k - i\frac{\Gamma}{2}} \left[e^{-i(\epsilon_2+\omega_k)t} - e^{-i\epsilon_3 t - \frac{\Gamma}{2}t} \right].$$

In order to study the system in the 2×2 subspace of the lower states, we take the limit $t \gg \Gamma^{-1}$. After the spontaneous emission process, the final state is a electron–photon wave-packet $\sum_{k;i=1,2} c_{ik}|i\rangle|k\rangle$, with the coefficients

$$c_{1k} \approx -\frac{g_{1k}}{\epsilon_3 - \epsilon_1 - \omega_k - i\frac{\Gamma}{2}} e^{-i(\epsilon_1+\omega_k)t}, \qquad (7)$$

$$c_{2k} \approx -\frac{g_{2k}}{\epsilon_3 - \epsilon_2 - \omega_k - i\frac{\Gamma}{2}} e^{-i(\epsilon_2+\omega_k)t}. \qquad (8)$$

The state of a photon is specified by its propagation direction $\mathbf{n}$, polarization $\sigma(\boldsymbol{\varepsilon}_\sigma \perp \mathbf{n})$, and frequency ω. So, we can formulate the total wave packet as

$$\sum_{\mathbf{n},\sigma} \left[g_{1\sigma} e^{-i\epsilon_1 t}|1\rangle|\mathbf{n},\sigma,f_1(t)\rangle + g_{2\sigma} e^{-i\epsilon_2 t}|2\rangle|\mathbf{n},\sigma,f_2(t)\rangle \right], \qquad (9)$$

where we have taken the coupling constants to be frequency-independent. In Eq. (9) $f_j(t)$ is the pulse shape of the photon. From Eqs. (7) and (8), we see that the photon wave packet has a finite bandwidth; this point, which was first studied by Weisskopf and Wigner in their classic treatment of spontaneous emission,[14] is reflected in the structure of $f_j(t)$. These functions have a central frequency equal to $\epsilon_3 - \epsilon_j$ and a bandwidth equal to Γ. As a consequence of the finite bandwidth, for a given propagation direction and polarization, the basis states $\{|\mathbf{n},\sigma,f_j\rangle\}$ are not orthogonal, the overlap between them being

$$\langle \mathbf{n},\sigma,f_l|\mathbf{n},\sigma,f_j\rangle = \frac{i\Gamma}{i\Gamma + \epsilon_{lj}}, \qquad (10)$$

where $\epsilon_{lj} = \epsilon_l - \epsilon_j$.

We should emphasize that the wave packet formed in Eq. (9) does not rely on the Markovian approximation. In a full quantum kinetic description of the photon emission process, the wave packet of the whole system would still have the same form, the central frequency and bandwidth of the pulses would be close to those found using the Markovian approximation, but the specific profile of $f_j(t)$ would be different from those given by Eqs. (7) and (8).

The various phenomena (electron and photon polarization entanglement, SGC, and two-pathway decay) can all be derived from the wave packet of Eq. (9).

If the spontaneously emitted photon is not detected at all, we have to average over the ensemble of photons of all possible propagation directions to obtain the electronic state. This is the usual textbook treatment of spontaneous emis-

sion. However, if detection of an emitted photon leads to a knowledge that its direction of propagation is $\mathbf{n}_0$, then the (unnormalized) electron-photon wave packet should be projected along that direction:

$$\sum_\sigma \left[g_{1\sigma} e^{-i\epsilon_1 t} |1\rangle |\mathbf{n}_0, \sigma, f_1(t)\rangle + g_{2\sigma} e^{-i\epsilon_2 t} |2\rangle |\mathbf{n}_0, \sigma, f_2(t)\rangle \right]. \tag{11}$$

When the two transitions are very close in frequency, i.e., $\eta \equiv |\epsilon_1 - \epsilon_2| / \Gamma \ll 1$, the overlap of the two photon wave packets deviates from unity by $\mathcal{O}(\eta)$. After tracing out the envelopes of the photon by use of any complete basis (e.g., monochromatic states), the state of the electron and photon polarization is, with the propagation direction $\mathbf{n}_0$ understood,

$$|Y\rangle = \sqrt{N} \sum_\sigma \left[g_{1\sigma} |1\rangle |\sigma\rangle + g_{2\sigma} |2\rangle |\sigma\rangle \right] + \mathcal{O}(\eta), \tag{12}$$

where N is a normalization constant, given by

$$N^{-1} = \sum_{j=1,2} \sum_{\sigma=\alpha,\beta} |g_{j\sigma}|^2. \tag{13}$$

The order η error recorded here is meant to indicate the magnitude of the *mixed-state* error which, if neglected, results in a pure state. From this pure state, we can find explicitly the necessary conditions for entanglement or SGC. However, the approximation of neglecting η is unnecessary for computing a measure of entanglement of the resultant mixed state.[15]

A. Entanglement

A measure of entanglement of the bipartite state $|Y\rangle$ in Eq. (12) is given by the von Neumann entropy of the reduced density matrix of the state[16] for either the subsystem E of the two low-lying electronic states or the subsystem P of the photon polarization states. Taking the partial trace of the polarization states of the density matrix $|Y\rangle\langle Y|$ of the pure state leads to the 2×2 reduced density matrix for the electronic states,

$$\rho_E = N \sum_{ij} |i\rangle \left[\sum_\sigma g_{i\sigma} g_{j\sigma}^* \right] \langle j|. \tag{14}$$

Diagonalization of this partial density matrix leads to two eigenvalues,

$$p_\pm = \frac{1}{2} \pm \sqrt{\frac{1}{4} - D^2}, \tag{15}$$

where D^2 is the determinant of the reduced density matrix ρ_E, or

$$D = N|g_{1\alpha} g_{2\beta} - g_{1\beta} g_{2\alpha}|, \tag{16}$$

for the two electronic state and two polarizations, α, β, normal to the propagation direction $\mathbf{n}_0$. The entropy of entanglement is given by the entropy,

$$S = -p_+ \log_2 p_+ - p_- \log_2 p_-. \tag{17}$$

As D ranges from 0 to $1/2$, the entropy ranges from 0 to 1 giving a continuous measure of entanglement as the state $|Y\rangle$

goes from no entanglement to maximum entanglement. To find the axis $\mathbf{n}_0$ along which the entanglement is maximum, we have to maximize D as a function of the orientation. For a particular system, this axis can be found in terms of the dipole matrix elements of the two transitions. However, not all systems can have maximally entangled states. We will apply this to specific examples in the following section.

B. SGC

From the reduced density matrix, we can also find the conditions for SGC. Maximum SGC occurs when the reduced density matrix is a pure state. In terms of the electron-photon coupling constants, the condition is the vanishing of the discriminant D in Eq. (16). This means that when the SGC effect is maximized, there exists a particular transformation which takes the basis of the electronic states $\{|1\rangle, |2\rangle\}$ to a basis $\{|\mathcal{B}\rangle, |\mathcal{D}\rangle\}$ which has the property that $|\mathcal{B}\rangle$ is always the final state of the Λ system immediately after the spontaneous emission process, and $|\mathcal{D}\rangle$ is a state disconnected from the excited state by dipolar coupling, i.e., a dark state. This point will be further explored in Sec. III. The extreme values of $D=0$ and $1/2$ make it clear that maximum SGC means no entanglement, and conversely that maximal entanglement leads to no SGC. However, partial entanglement can coexist with the potentiality of some SGC for values of D between the two extremes.

Our theory can be easily extended to systems with more than two ground states. For example, in a system whose ground states are the four states from two electron spins, the SGC may lead to the coherence and entanglement between the two spins, which is the mechanism of a series of proposals of using vacuum fluctuation to establish entanglement between qubits[17,18].

C. Two-pathway decay

So far, we have investigated the consequences when the two transitions are close in frequency ($\eta \ll 1$). When this is not the case, the tracing out of the wave packet will generally produce a mixed state in electron spins and photon polarizations. In the limit of large η, i.e., $|\epsilon_2 - \epsilon_1| \gg \Gamma$, the overlap between the two photon wave functions, $\langle f_1(t)|f_2(t)\rangle \simeq 0$, and the reduced density matrix for the spin and photon polarization would be mixed. In this case, there is neither spin-polarization entanglement nor SGC, but instead the time development can be described as a two-pathway decay process: The excited state can relax to two different states by the emission of photons with distinct frequencies. For η between these two limits, the state in Eq. (11) may lead to an entanglement between the pulse shapes of the photon and the two lower electronic levels on measuring the photon polarization. Furthermore, from the entangled state in Eq. (11), SGC or polarization entanglement may still be recovered (provided of course that the necessary conditions on the g's are satisfied) if the quantum information carried by the frequency of the photon is erased[19]. This can be done by chopping part of the photon pulse, and thus subjecting its frequency to (more) uncertainty. In a time-selective

measurement, only photons emitted at a specific time period, say from t_0 to t_0+dt, are selected. So the projection operator associated with this measurement is $p_0=|\delta(t-t_0)\rangle\langle\delta(t-t_0)|$, which represents a δ photon pulse passing the detector at $t=t_0$. The projected state after this measurement

$$\sum_\sigma \left[g_{1\sigma} f_1(t_0)|1\rangle + g_{2\sigma} f_2(t_0)|2\rangle \right]|\mathbf{n}_0\sigma\rangle \qquad (18)$$

is a pure state of the electron and photon polarization, so that entanglement or SGC is restored. By writing the projector in the frequency domain

$$\tilde{P}_0 = \int d\omega \int d\omega' e^{i(\omega-\omega')t_0}|\omega'\rangle\langle\omega|, \qquad (19)$$

we see that it can be understood as a broadband detector with definite phase for each frequency channel; thus, it can erase the frequency (which path) information while retaining the phase correlation. We note that a usual broadband detector without phase correlation is not sufficient to restore the pureness of the state. It is also interesting that SGC and entanglement can be controlled by choosing a different detection time t_0, as seen from Eq. (18).

III. SYMMETRY CONSIDERATIONS FOR SGC

In this section, we investigate the symmetry relations between the different parts of the Hamiltonian necessary for SGC terms to appear. Our treatment is not restricted to Λ systems, but can be extended to a system with more than two lower levels.

Consider a quantum mechanical system with one higher-energy level $|e\rangle$ and a set of lower-lying states, described by a Hamiltonian H°. Taking into account only dipole-type interactions, denote by $\mathcal{J}_z$ the polarization operator used in the selection rules. The z axis is defined by the excited state via

$$\mathcal{J}_z|e\rangle = M_e|e\rangle.$$

Note that $\mathcal{J}_z$ can be either J_z, where $\mathbf{J}=\mathbf{L}+\mathbf{S}$ is the total angular momentum operator and $\mathbf{S}$ is the spin, or L_z, as determined by the condition

$$[\mathcal{J}_z, H^\circ] = 0.$$

That is to say that there is an axial symmetry in the system associated with $\mathcal{J}_z$. Among the lower lying states, the ones of interest are the ones appearing in the final entangled state $|\Upsilon\rangle$ of the whole system. We will refer to these states as "bright", because they are orthogonal to the familiar dark states from quantum optics. There are at most three such states, $\{\mathcal{B}_j\}$, within a given degenerate manifold, corresponding to the three different possible projections of the dipole matrix elements along the z axis, so $j=1,0,\bar{1}$. In general, not all systems will have all three bright states. This concept that the final state involves only a small number of states (three in our case), gives a physical understanding of the electron-photon entangled state.[20]

In order to have SGC, i.e., one or more terms of the type $\dot{\rho}_{jk}=\Gamma\rho_{ee}$, with $j\neq k$ and $j,k\neq e$, there has to be a perturba-

tion H^B that breaks the symmetry associated with $\mathcal{J}_z$; in particular, the following conditions have to be satisfied:

1. $[H^B, \mathcal{J}_z] \neq 0$;
2. $H^B|e\rangle \propto |e\rangle$;
3. $|\epsilon_{12}| \lesssim \Gamma$.

In general, we expect SGC between two eigenstates of the Hamiltonian $H=H^\circ+H^B$ which have nonzero overlap with the same bright state. The role of the first condition is to make SGC nontrivial; without this condition, it would always be possible to rotate to a different basis and formally acquire an SGC-like term in the equations (e.g., by rotating to the x basis in the zero-magnetic field case in the heavy-hole trion system discussed below). The second condition ensures that the excited state will not mix under the action of H^B; relaxing this condition gives rise to the Hanle effect,[9,12] in which an ensemble of atoms in a magnetic field is illuminated with an x-polarized pulse and the reradiated light may be polarized along y. This effect is another example where coherence plays an important role; it has recently been observed in doped GaAs quantum wells, in the heavy-hole trion system with confinement in one dimension.[21] We shall discuss the quantum dot case below. As shown in Sec. II, when the radiative linewidth of the excited state is smaller than the energy differences of the lower states the SGC effect will be averaged out. The third condition provides the valid regime for the occurrence of this phenomenon.

The perturbation H^B can be realized by a static electric or magnetic field, by the spin-orbit coupling, hyperfine coupling, etc. Note the different origins of H^B in different systems and that it may or may not be possible to control H^B. Examples of various systems follow, exhibiting the above conditions and demonstrating the different origins of H^B.

IV. EXAMPLES FROM ATOMIC PHYSICS

A. SGC in atoms

Consider an atom with Hamiltonian H°; excluding relativistic corrections, it can be diagonalized in the $|N,L,S,M_L,M_S\rangle$ basis. Consider as the system of interest the subspace of H° formed by $|N,1,1,1,1\rangle=|e\rangle$ and the lower-energy states $|N-1,L,S,M_L,M_S\rangle$. The various quantum numbers are, of course, restricted by selection rules, and $\mathcal{J}_z=L_z$. Here, we will list only the three bright states:

$$|\mathcal{B}_1\rangle = |N-1,2,1,2,1\rangle,$$

$$|\mathcal{B}_0\rangle = |N-1,2,1,1,1\rangle,$$

$$|\mathcal{B}_{\bar{1}}\rangle = a|N-1,2,1,0,1\rangle + b|N-1,0,1,0,1\rangle.$$

where the coefficients a and b can be determined in the following way. In the original $|NJM_JLS\rangle$ basis, the matrix elements for the transitions $|N-1,2,1,0,1\rangle\leftrightarrow|N,1,1,1,1\rangle$ and $|N-1,0,1,0,1\rangle\leftrightarrow|N,1,1,1,1\rangle$ are given by the Wigner–Eckart theorem. By rotating to the $\{|\mathcal{B}\rangle,|\mathcal{D}\rangle\}$ basis, and requiring the transition $|\mathcal{D}\rangle\leftrightarrow|N,1,1,1,1\rangle$ to be forbidden, we find a and b. Inclusion of the spin-orbit interaction, which plays the role of H^B, i.e., $H^B=\alpha\mathbf{L}\cdot\mathbf{S}$, condition (i) is satisfied, the eigenstates of H^B being $|NJM_JLS\rangle$. Condition (ii) is also

satisfied, because $|e\rangle$, as the state of maximum M_L and M_S, does not mix under the spin-orbit coupling. In the new basis, SGC is expected to occur between states with the same value of M_J, which can also be verified by direct calculation. In this example, the linewidth of $|e\rangle$ is much smaller than the spin-orbit coupling strength α. Typical values in atoms are $\Gamma_e \sim 1\ \mu\,\text{eV}$ and $\alpha \sim 1\ \text{meV}$, which means that SGC will not be observed in such a system.

B. Entanglement and SGC of atomic hyperfine states

In this example, the Λ system is formed by the hyperfine states of a single trapped Cd ion in the presence of a magnetic field along the z axis. In the $|FM_F\rangle$ basis, the excited state is $|21\rangle$ and the two lower levels are $|11\rangle$ and $|10\rangle$. The two lower levels have the same principle quantum number N. The entanglement between the polarization of the photon and the atom has been demonstrated experimentally.[8] To illustrate the methods developed in Sec. II, we will make use of the fact that the two lower levels are states of definite angular momentum and its projection to the z axis. Then, by the Wigner–Eckart theorem we know that the dipole moment of the transition $|21\rangle \rightarrow |10\rangle$ has a nonzero component only along $\mathbf{e}_+ = \mathbf{x} + i\mathbf{y}$ whereas that of $|21\rangle \rightarrow |11\rangle$ has only a component along $\mathbf{z}$. The wave packet of the system is then given by

$$|\Upsilon\rangle = \frac{-\sqrt{2}\sin\vartheta|\vartheta\rangle|11\rangle + e^{-i\varphi}\cos\vartheta|\vartheta\rangle|10\rangle - ie^{-i\varphi}|\varphi\rangle|10\rangle}{\sqrt{2 + \sin^2\vartheta}},$$
(20)

where ϑ and φ are the spherical coordinates measured from z and x axis, respectively, and $|\vartheta\rangle$ and $|\varphi\rangle$ are the polarization basis states, which are linearly polarized parallel and normal to the plane formed by the z axis and the propagation direction, respectively. Then, from Eq. (20), we read off the g's:

$$g_{1\vartheta} \propto -\sqrt{2}\sin\vartheta,$$
(21)

$$g_{1\varphi} = 0,$$
(22)

$$g_{2\vartheta} \propto e^{-i\varphi}\cos\vartheta,$$
(23)

$$g_{2\varphi} \propto ie^{-i\varphi},$$
(24)

where $|11\rangle \equiv |1\rangle$ and $|10\rangle \equiv |2\rangle$. The measure of entanglement by D is

$$D = \frac{\sqrt{2}\sin\vartheta}{\sqrt{2 + \sin^2\vartheta}}.$$
(25)

The maximum possible entanglement occurs at $\vartheta = \pi/2$, i.e., whenever the photon propagates perpendicularly to z. The maximum value of 0.47 is close to being maximally entangled. D does not depend on φ, as expected since there is azimuthal symmetry about z.

In terms of SGC and symmetry, it is interesting to notice that the role of the (external or internal) field, H^B, introduced in Sec. III can be played by the different projections (measurements) because the state before the measurement is an eigenstate of the operator J_z (total angular momentum along z), but not after the measurement in general. The magnetic field along the z axis is included in the Hamiltonian H°. If the spontaneously emitted photons are measured along the quantization axis, only the ones emitted from the transition $|21\rangle \rightarrow |10\rangle$ will be detected, since only their polarization allows propagation along z. On the other hand, a photon detector placed at a finite angle from z can play the role of H^B. Suppose a photon is spontaneously emitted along an axis $n = (\vartheta, \varphi)$. The density matrix of the state given by Eq. (20) is $|\Upsilon\rangle\langle\Upsilon|$. If we are only interested in the dynamics of the ion, and the polarization of the photon is not measured, then the photon polarization has to be traced out. Then the reduced density matrix of the system in the atomic states is

$$\rho_E = \frac{1}{2 + \sin^2\vartheta}\begin{bmatrix} \cos^2\vartheta + 1 & \sqrt{2}e^{-i\varphi}\cos\vartheta\sin\vartheta \\ \sqrt{2}e^{+i\varphi}\cos\vartheta\sin\vartheta & 2\sin^2\vartheta \end{bmatrix}.$$
(26)

The off-diagonal elements express coherence between the hyperfine states with dependence on the photon propagation direction. We can check that for $\vartheta = 0$ the probability of the atom being in the $|11\rangle$ state is zero and there are no off-diagonal elements, and for $\vartheta = \pi/2$ the off-diagonal elements are also zero, which means there is no SGC, but the state has the maximum possible entanglement. For all the intermediate values of ϑ, the hyperfine states and the photon polarization are entangled, and there is also some SGC when the photon is traced out. Maximum SGC occurs when D is minimized; from Eq. (25) we see that it is zero for $\vartheta = 0$. This is expected anytime one of the two transitions involves a linearly polarized photon, since the latter cannot propagate along the quantization axis. So, for this orientation, the final state can only be $|10\rangle$. For intermediate angles, for instance $\vartheta = \pi/4$, there is both entanglement and SGC involving both lower states, when the photon is traced out. Since SGC only occurs for particular photon propagation directions, we could view it as "probabilistic" SGC.

V. EXAMPLES FROM SOLID-STATE PHYSICS

A. Heavy-hole trion system in a magnetic field

In the optical control of the electron spin in a doped quantum dot,[4] a static magnetic field is imposed in a fixed direction at an angle ψ with respect to the propagation of the circularly polarized pulse along the growth direction of the dot, defined as the z axis. The two eigenstates of the electron spin along the field direction and the intermediate trion (bound state of an exciton with the excess electron) state in the Raman process form a three-level Λ system. The trion state of interest consists of a p-like heavy hole and a pair of electrons in the singlet state. The g-factor in the xy plane of the heavy hole is approximately zero in magnetic fields up to 5 T (Ref. 22), and the two electrons are in a rotationally invariant state. This means that the trion state, although it is spin polarized along z, will not precess about a perpendicular B field. Therefore, it can be described by the "good" quantum numbers $J = 3/2$ and its projection along z, $M_J = 3/2$. The lower levels $|1\rangle, |2\rangle$ are the eigenstates of the spin along the

direction of the *B* field and have $j=1/2$ and $m_j=1/2,-1/2$, respectively.

To check if this system will have SGC, we will examine whether the conditions of Sec. III are satisfied. We take $H°$ to be the Hamiltonian of the quantum dot, with $|e\rangle=|\tau\rangle$, the trion state described above, excited by $\sigma+$light; $\mathcal{J}_z=J_z$, since the spin-orbit interaction is included in $H°$, and any component of the *B* field along *z* can also be included. H^B is the contribution to the Hamiltonian due to the magnetic field along *x*. Condition (1) is fulfilled since $g_x\simeq0$, and condition (2) is obviously satisfied. The only bright state is the electron spin s_z eigenstate, $|z\rangle\equiv|\uparrow\rangle$. For later use, we also define $|\bar{z}\rangle\equiv|\downarrow\rangle$. Therefore, we expect SGC between states $|1\rangle$ and $|2\rangle$ for any angle ψ, and since the linewidth of the trion is large enough compared to the Zeeman splitting, SGC should moreover have a detectable effect. As a matter of fact, it has already been demonstrated experimentally for this system, and, to the best of our knowledge, it is the only direct observation of SGC.[13] For this nonlinear pump-probe experiment, the inclusion of SGC into the equations causes the amplitude and the phase of the probe signal to depend on the Zeeman splitting. More details on how this dependence occurs will be presented in the following section.

Although our discussion has focused on single Λ systems, the experiment was carried out for an ensemble. In general, for an ensemble of equivalent noninteracting atoms, an average over the different *z* axes would have to be performed. However, in this quantum-dot solid-state system, there is a common *z* axis for all the dots, since they are grown on the same plane (xy), and they have a relatively large in-plane cross-section as compared to their height. This is a clear advantage of the quantum-dot ensemble over an ensemble of atoms.

We can also analyze this system using the methods in Sec. II. To find the *g*'s, we need the dipole matrix elements. These can be found by writing

$$|1\rangle = \cos\frac{\psi}{2}|\uparrow\rangle + \sin\frac{\psi}{2}|\downarrow\rangle, \tag{27}$$

$$|2\rangle = \sin\frac{\psi}{2}|\uparrow\rangle - \cos\frac{\psi}{2}|\downarrow\rangle. \tag{28}$$

Again, we will make use of the fact that $|\uparrow\rangle$ and $|\tau\rangle$ are angular momentum eigenstates along the *z* axis, with the familiar selection rules. Only state $|\uparrow\rangle$ has a nonzero dipole matrix element with $|\tau\rangle, d_+\mathbf{e}_+$, so that the transitions $|1\rangle\rightarrow|\tau\rangle$ and $|2\rangle\rightarrow|\tau\rangle$ have dipole matrix elements equal to $d_+\cos\frac{\psi}{2}\mathbf{e}_+$ and $d_+\sin\frac{\psi}{2}\mathbf{e}_+$ respectively. Then, for a photon emitted along $\mathbf{n}_0=(\vartheta,\varphi)$, we find the couplings:

$$g_{1\vartheta} = d_+e^{i\varphi}\cos\vartheta\cos\frac{\psi}{2}, \tag{29}$$

$$g_{1\varphi} = d_+ie^{i\varphi}\cos\frac{\psi}{2}, \tag{30}$$

$$g_{2\vartheta} = d_+e^{i\varphi}\cos\vartheta\sin\frac{\psi}{2}, \tag{31}$$
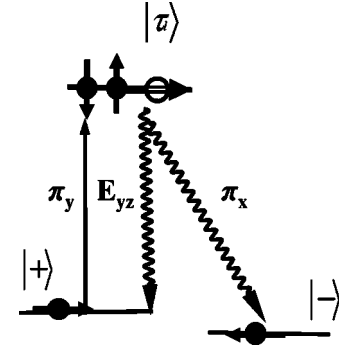

FIG. 1. The energy levels of the Λ system consisting of the two electron spin states (lower levels) and the light-hole trion polarized along the $+x$ direction. The solid line represents the laser pulse, which propagates along *z* and is linearly polarized in the *y* direction. The wavy lines denote the spontaneously emitted photons from the transitions $|\tau_l\rangle\rightarrow|+\rangle$ and $|\tau_l\rangle\rightarrow|-\rangle$, which are elliptically polarized in the *yz* plane and linearly polarized along *x*, respectively.

$$g_{2\varphi} = d_+ie^{i\varphi}\sin\frac{\psi}{2}, \tag{32}$$

so that the determinant is always zero, independent of $\mathbf{n}_0$. This means that the system in this configuration will never be entangled with the polarization of the photon, which, as we have seen, implies maximum SGC. The final state of the Λ system is always $|\uparrow\rangle$, unentangled. Section VI gives an intuitive picture of this concept by the vector representation of (the mean value of) the spin.

B. Light-hole trion in Voigt configuration

The spin-photon entanglement can be also realized in a quantum-dot system by employing the light-hole trion state. The heavy-and light-hole excitons are split by the breaking of the tetrahedral symmetry of the bulk III-V compound. It might also be possible to make the light-hole states lower in energy than the heavy holes. The magnetic field is pointing along the *x* direction, so that the lower levels are the two S_x eigenstates, $|+\rangle$ and $|-\rangle$. The optical pulses used are such that the light-hole trion polarized along the $+x$ direction is excited. The excited state is a trion of a singlet pair of electrons and a light hole which is in the $m_j=\pm1/2$ component of the $j=3/2$ state. The trion can thus be characterized by the state $|JM_J\rangle=|3/2,\pm1/2\rangle$. We choose the $M_J=1/2$ state as the excited state of the Λ system and denote it by $|\tau_l\rangle$.

The transitions $|\tau_l\rangle\rightarrow|+\rangle$ and $|\tau_l\rangle\rightarrow|-\rangle$ involve a photon linearly polarized along *x* ($|X\rangle\equiv|\pi_x\rangle$)) and one with elliptical polarization ($-i|Y\rangle+2|Z\rangle\equiv|E_{yz}\rangle$)), respectively (see Fig. 1).[23] In particular, after $|\tau_l\rangle$ has decayed, the state of the system is from Eq. (12),

$$|Y\rangle = -\frac{1}{\sqrt{6}}[|X\rangle|-\rangle + (2|Z\rangle - i|Y\rangle)|+\rangle], \tag{33}$$

We assume a measurement which determines the propagation direction of the photon $\mathbf{n}_0=(\vartheta,\varphi)$. Then the state becomes:

$$|\Upsilon\rangle = \frac{-1}{\sqrt{2+3\sin^2\vartheta}}[\cos\vartheta\cos\varphi|\vartheta\rangle|-\rangle$$
$$-(2\sin\vartheta+i\sin\varphi\cos\vartheta)|\vartheta\rangle|+\rangle$$
$$-\sin\varphi|\varphi\rangle|-\rangle-i\cos\varphi|\varphi\rangle|+\rangle]. \qquad (34)$$

Following the same procedure as in the trapped ion example, we find that the condition for maximum entanglement is $\vartheta = 0$; the value of D is then 0.5, maximal entnaglement. SGC will only occur when D in Eq. (16) is less than 0.5 and it will be maximum for propagation along x, which means that the electron will be in the state $|+\rangle$. For all other values of ϑ, there will be both entanglement and SGC between the two energy eigenstates when the photon is traced out. The phenomena following the spontaneous radiative decay of this system are indeed very similar to the trapped ion case. In the solid-state system, there is no need to isolate a single dot in order to observe SGC since all dots are oriented in the same direction.

For quantum information processing, entanglement between photon polarization and spin has to be established in a quantum dot. So isolating and addressing a single dot is required. Experimentally, this requirement is arguably feasible.[24] The system should be initialized at state $|+\rangle$ (or $|-\rangle$) and subsequently excited by y- (or x-) polarized light, so that only state $|\tau_l\rangle$ gets excited. Other trion states, involving electrons in the triplet state and/or heavy holes, have an energy separation from $|\tau_l\rangle$ large enough compared to the pulse bandwidth and so they can be safely ignored. Above, we found that the state will be maximally entangled when the spontaneously emitted photon propagates along z. When the optical axis is along z, the spontaneously emitted photon may be distinguished from the laser photons by optical gating. As an alternative to the optical gating, to minimize scattered light the detector may be placed along y, i.e., at $(\vartheta,\varphi) = (\pi/2,\pi/2)$. The value of D is then 0.2, so that the entanglement will be significantly less than that along the optical axis, but should be measurable. The observation of the emitted photon and the measurement of its polarization can be made as in Ref. 8. By use of the pump-probe technique, the state of the spin will also be measured to show the correlation with the polarization of the photon.

To overcome the probabilistic nature of the entanglement (as projection is needed) and to improve the quantum efficiency degraded by the scattering problem, cavities and waveguides may be employed to enhance and select desired photon emission processes.[7,25]

VI. PUMP-PROBE EXPERIMENT FOR SGC DETECTION IN A QUANTUM DOT

In this section, we provide a theoretical analysis for the pump-probe experiment which explicitly demonstrated SGC.[13] The Λ system is the heavy-hole trion system introduced above. We present a treatment based on the idea that SGC may be viewed as a decay to one bright state which is a superposition of the eigenstates. The vector character of the mean value of the spin, which also helps develop intuition for the SGC effect, is employed and in fact it anticipates
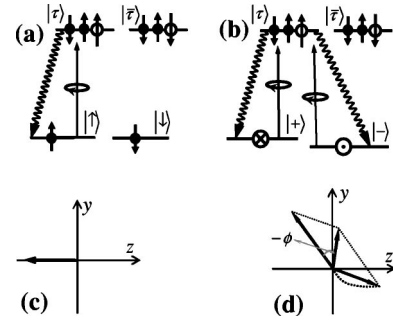

FIG. 2. (a) and (b) are the energy diagrams and possible electron-trion transitions caused by $\sigma+$-polarized photons with the electron spin quantized in z and x directions, respectively. (c) The Raman coherence generated by the pump pulse, and (d) Schematic depiction of interference between the Raman coherence and the spin coherence generated by spontaneous emission, under a magnetic field applied along the x direction.

some of the theoretical results of the pump-probe measurements calculated by perturbative solution of the density matrix in the remainder of this section.

A. Geometrical picture of SGC

As shown by Bloch[26] and Feynman *et al.*,[27] an ensemble of two-level systems can be described by a rotating vector. This picture provides an intuitive understanding of the spin coherence generated by the optical excitation and spontaneous decay of the trion states. For simplicity, we will assume the short-pulse limit in this section.

Regardless of the presence or absence of the magnetic field, there is freedom in the choice of the quantization direction, and it is convenient in this case to choose the spin eigenstates quantized in the growth (z) direction, $|\uparrow\rangle$ and $|\downarrow\rangle$. The two trion states $|\tau\rangle$ and $|\bar\tau\rangle$ have $J=3/2$ and z-component $M=+3/2$ and $M=-3/2$, respectively. The selection rules are such that a photon with helicity ±1 ($\sigma\pm$ circular polarization) excites the electron $|\uparrow\rangle$ or $|\downarrow\rangle$ to the trion states $|\tau\rangle$ or $|\bar\tau\rangle$, respectively. We will consider a $\sigma+$ polarized pump, which excites spin-up electrons to the trion state $|\tau\rangle$, leaving the electron spin polarized in the $-z$ direction. Due to the selection rules, the trion state can only relax back to the spin-up state by emitting a $\sigma+$ polarized photon, and after recombination, the electron remains unpolarized.

Now let us consider a strong magnetic field, applied at $\psi=\pi/2$ with respect to the optical axis, $\boldsymbol{B}=B\mathbf{e}_x$. In this so-called Voigt configuration, the Zeeman states $|\pm\rangle \equiv (|\uparrow\rangle\pm|\downarrow\rangle)/\sqrt{2}$ are quantized in the x direction and are energy eigenstates with energies $\pm\omega_L$, respectively, while the trion states can still be assumed quantized in the z direction [see Fig. 2(b)]. Note that the low-lying states $|1\rangle,|2\rangle$ in foregoing sections are now denoted by the spin states, $|+\rangle,|-\rangle$. In the short-pulse limit, the pulse spectrum is much broader than the spin splitting or, equivalently, the pulse duration is much shorter than the spin precession period, so the excitation process is virtually unaffected by the magnetic field: the $\sigma+$ polarized pump excites the $|\uparrow\rangle$ electron to the trion state $|\tau\rangle$, leaving the electrons spin polarized in the $-z$ direction, as

in the zero-field case [see Fig. 2(c)]. The pulse generates coherence between the two eigenstates $|+\rangle$ and $|-\rangle$, which is the conventional Raman coherence[28] generated by a pulse with a spectrum broad enough to cover both the near-degenerate transitions. The spin precesses in the magnetic field normal to the plane of precession with frequency ω_L/π. In other words, the state oscillates between the spin-up and -down states. The Raman coherence can be determined by the excitation-induced change of the population in the spin state $|\uparrow\rangle$,

$$\rho_{\uparrow\uparrow}^R(t) = -\frac{\rho_{\tau\tau}}{2}\left[1 + \cos(2\omega_L t)e^{-\gamma_2 t}\right], \tag{35}$$

where $\rho_{\tau\tau}$ is the population of the trion state immediately after the excitation pulse, and γ_2 is the damping rate of the spin polarization (due to spin dephasing and inhomogeneous broadening).

On the other hand, when the system is in the trion state $|\tau\rangle$, the trion will relax by emitting a $\sigma+$-polarized photon, leaving an electron spin polarized in the $+z$ direction, i.e., generating coherence between the two spin eigenstates (SGC). The trion decay can be treated as a stochastic quantum jump process with the jump rate 2Γ. After the quantum jump, the evolution of the system can be described by a spin vector rotating under the transverse magnetic field. Thus, the spin polarization generated by the spontaneous emission during $[t', t'+dt']$ can be determined by

$$d\rho_{\uparrow\uparrow}^{SGC}(t,t') = \frac{\rho_{\tau\tau}e^{-2\Gamma t'}2\Gamma dt'}{2}\left[1 + \cos(2\omega_L(t-t'))e^{-\gamma_2(t-t')}\right]. \tag{36}$$

The precessing spin vector is deformed by the accumulation of increments through the optical decay into a spiral curve [see Fig. 2(d)]. The accumulated spin polarization due to the spontaneous emission is

$$\rho_{\uparrow\uparrow}^{SGC}(t) = \int_0^t d\rho_{\uparrow\uparrow}^{SGC}(t,t')$$

$$= \frac{\rho_{\tau\tau}}{2}\Re\left[1 - e^{-2\Gamma t} + \frac{2\Gamma}{2\Gamma - \gamma_2 - i2\omega_L}\right.$$
$$\left. \times (e^{-i2\omega_L t-\gamma_2 t} - e^{-2\Gamma t})\right]. \tag{37}$$

For an initially unpolarized system, the total spin polarization in the z direction after the action of the pump and the recombination process is given by

$$\rho_{\uparrow\uparrow}^{(2)} = \left[\rho_{\uparrow\uparrow}^R + \rho_{\uparrow\uparrow}^{SGC}\right]$$

$$= -\frac{\rho_{\tau\tau}}{2}\left[(1 + a_\Gamma)e^{-2\Gamma t} + a_0\cos(2\omega_L t - \phi)e^{-\gamma_2 t}\right], \tag{38}$$

where

$$a_\Gamma \equiv \frac{2\Gamma(2\Gamma - \gamma_2)}{(2\Gamma - \gamma_2)^2 + 4\omega_L^2}, \tag{39}$$

$$a_0 \equiv \sqrt{\frac{\gamma_2^2 + 4\omega_L^2}{(2\Gamma - \gamma_2)^2 + 4\omega_L^2}}, \tag{40}$$

$$\phi \equiv -\arctan\frac{2\Gamma - \gamma_2}{2\omega_L} - \arctan\frac{\gamma_2}{2\omega_L}. \tag{41}$$

As shown in Fig. 2(d), SGC induces a phase shift of the spin coherence as compared to the Raman coherence. Note also the different amplitudes of the Bloch vectors in the case with and without SGC. We can see that if the recombination is much faster than the spin precession under the magnetic field, i.e., $\Gamma \gg \omega_L$, SGC actually cancels the Raman coherence. This is not surprising since such a limit simply corresponds to the zero-field case. In the strong field limit where $\omega_L \gg \Gamma$, the spin precession will average SGC to zero, which corresponds to the two-pathway decay discussed in Sec. II. From Eq. (36), it can be seen that at any specific time the trion relaxes to state $|\uparrow\rangle$, so, as shown in Sec. II, a time-selective measurement can recover the SGC from the incoherent two-pathway decay. Without such a projection, as the spin coherence generated at a different time has a different phaseshift, the time averaging [see Eq. (37)] leads to the vanishing of the SGC.

In a pump-probe experiment, what is measured is the differential transmission signal (DTS), i.e., the difference between the probe transmission with and without the pump pulse. In the same-circular polarization (SCP) pump-probe configuration, the probe measures the change in the population difference created by the pump, $\rho_{\tau\tau} - \rho_{\uparrow\uparrow}^{(2)}$. Hence, the DTS is given by

$$\Delta T^{SCP} \propto (3 + a_\Gamma)e^{-2\Gamma t_d} + a_0\cos(2\omega_L t_d - \phi), \tag{42}$$

where t_d is the delay time between the pump and probe pulses. The DTS reveals the spin beatings and the SGC effect manifests itself in the dependence of the beat amplitude and phase shift on the strength of the magnetic field.

The pump-probe experiment can also be done in the opposite circular polarization (OCP) configuration. The probe measures the change of population of the spin-down state $|\downarrow\rangle$. The DTS in this case is proportional to $-\rho_{\downarrow\downarrow}^{(2)} = \rho_{\uparrow\uparrow}^{(2)} + \rho_{\tau\tau}$, i.e.,

$$\Delta T^{OCP} \propto (1 - a_\Gamma)e^{-2\Gamma t_d} - a_0\cos(2\omega_L t_d - \phi). \tag{43}$$

The spin beat has the opposite sign to the SCP case.

Similar analysis shows that if either the pump or the probe pulse is linearly polarized, there will be no spin beat in the DTS.

B. Perturbative solution of the probe signal

The optical field of the pump and probe pulses can be written as

$$\mathbf{E}(t) = (\mathbf{e}_+ E_{1+} + \mathbf{e}_- E_{1-})\chi_1(t)e^{-i\Omega_1 t}$$
$$+ (\mathbf{e}_+ E_{2+} + \mathbf{e}_- E_{2-})\chi_2(t-t_d)e^{-i\Omega_2(t-t_d)}, \tag{44}$$

where the subscripts 1 and 2 denote the pump and probe pulses, respectively, and $\mathbf{e}_\pm$ are the unit vectors of the $\sigma\pm$ polarizations. The dipole operator is

$$\hat{\mathbf{d}} = d(\mathbf{e}_+|\tau\rangle\langle\mp| \pm \mathbf{e}_-|\vec{\tau}\rangle\langle\pm|) + \text{h.c.}$$

Thus, in the rotating wave approximation, the Hamiltonian in the basis $\{|-\rangle, |+\rangle, |\tau\rangle, |\vec{\tau}\rangle\}$ can be written in matrix form as

$$H = \begin{bmatrix} -\omega_L & 0 & -d^*E_+^*(t) & -d^*E_-^*(t) \\ 0 & \omega_L & -d^*E_+^*(t) & +d^*E_-^*(t) \\ -dE_+(t) & -dE_+(t) & \epsilon_g & 0 \\ -dE_-(t) & +dE_-(t) & 0 & \epsilon_g \end{bmatrix}, \tag{45}$$

where ϵ_g is the energy of the trion states, and γ_1, γ_2, and 2Γ denoting the spin-flip rate, the spin-depolarizing rate, and the trion decay rate, respectively. The explicit equations for each element of the density matrix are

$$\dot{\rho}_{\tau,+} = i[\rho, H]_{\tau,+} - \Gamma\rho_{\tau,+}, \tag{46}$$

$$\dot{\rho}_{\tau,-} = i[\rho, H]_{\tau,-} - \Gamma\rho_{\tau,-}, \tag{47}$$

$$\dot{\rho}_{+,+} = i[\rho, H]_{+,+} - \gamma_1\rho_{+,+} + \Gamma(\rho_{\tau\tau} + \rho_{\vec{\tau}\vec{\tau}}), \tag{48}$$

$$\dot{\rho}_{-,-} = i[\rho, H]_{-,-} + \gamma_1\rho_{+,+} + \Gamma(\rho_{\tau\tau} + \rho_{\vec{\tau}\vec{\tau}}), \tag{49}$$

$$\dot{\rho}_{+,-} = i[\rho, H]_{+,-} - \gamma_2\rho_{+,-} + \Gamma_c(\rho_{\tau\tau} - \rho_{\vec{\tau}\vec{\tau}}), \tag{50}$$

$$\dot{\rho}_{\tau\tau} = i[\rho, H]_{\tau\tau} - 2\Gamma\rho_{\tau\tau}, \tag{51}$$

$$\dot{\rho}_{\vec{\tau},t} = i[\rho, H]_{\vec{\tau},t} - 2\Gamma\rho_{\vec{\tau},t}, \tag{52}$$

$$\dot{\rho}_{\vec{\tau}\vec{\tau}} = i[\rho, H]_{\vec{\tau}\vec{\tau}} - 2\Gamma\rho_{\vec{\tau}\vec{\tau}}. \tag{53}$$

The Markov–Born approximation for the system photon has been employed. The term representing the spontaneously

generated spin coherence due to the trion recombination is indicated by the suffix c; Γ_c should be equal to Γ. However, we singled out the SGC term so that Γ_c can be artificially set to zero for a theoretical comparison between the results with and without the SGC effect.

In the pump-probe experiment, the DTS corresponds to the third-order optical response. The absorption of the probe pulse is proportional to the work W done by the probe pulse, and the DTS is[29]

$$\Delta T \propto -W^{(3)} = -2\mathfrak{R} \int \dot{\mathbf{P}}^{(3)}(t) \cdot \mathbf{E}_2^*(t - t_d)$$

$$\approx -2\Omega_2\mathfrak{J} \int \widetilde{\mathbf{P}}^{(3)}(\omega + \Omega_2) \cdot \widetilde{\mathbf{E}}_2^*(\omega + \Omega_2)\frac{d\omega}{2\pi}. \tag{54}$$

The third-order optical polarization of the system can be calculated directly by expanding the density matrix according to the order of the optical perturbation

$$\mathbf{P}^{(3)} = \mathbf{e}_+ d[\rho_{\tau,-}^{(3)} + \rho_{\tau,+}^{(3)}] + \mathbf{e}_- d[\rho_{\vec{\tau},-}^{(3)} - \rho_{\vec{\tau},+}^{(3)}], \tag{55}$$

Thus, given the σ+-polarized pump pulse, the third-order polarization in the SCP and OCP cases can be respectively calculated as[29]

$$\mathbf{P}_{\text{SCP}}^{(3)}(t) = \mathbf{e}_+ d[\rho_{\tau,-}^{(3)}(t) + \rho_{\tau,+}^{(3)}(t)], \tag{56}$$

$$\mathbf{P}_{\text{OCP}}^{(3)}(t) = \mathbf{e}_- d[\rho_{\vec{\tau},-}^{(3)}(t) - \rho_{\vec{\tau},+}^{(3)}(t)]. \tag{57}$$

C. Analytical results

The density matrix can be calculated straightforwardly order by order with respect to the pulse. Taking the initial state of the system to be the equilibrium state $\rho^{(0)} = \rho_+^{(0)}|+\rangle\langle+| + \rho_-^{(0)}|-\rangle\langle-|$. The result for the second-order spin coherence due to the pump pulse $\mathbf{E}_1(t)$ is:

$$\widetilde{\rho}_{+-}^{(2)}(\omega) = +X_1\frac{\rho_-^{(0)}}{\omega - 2\omega_L + i\gamma_2}\int_{-\infty}^{+\infty}\frac{\chi_1^*(\omega' - \omega)\chi_1(\omega')}{\omega' - \Delta_1 - \omega_L + i\Gamma}\frac{d\omega'}{2\pi} - X_1\frac{\rho_+^{(0)}}{\omega - 2\omega_L + i\gamma_2}\int_{-\infty}^{+\infty}\frac{\chi_1(\omega' + \omega)\chi_1^*(\omega')}{\omega' - \Delta_1 + \omega_L - i\Gamma}\frac{d\omega'}{2\pi}$$

$$+ X_1\frac{i\Gamma_c\rho_\pm^{(0)}}{(\omega - 2\omega_L + i\gamma_2)(\omega + i2\Gamma)}\int_{-\infty}^{+\infty}\frac{\chi_1(\omega' + \omega)\chi_1^*(\omega')}{\omega' - \Delta_1 \pm \omega_L - i\Gamma}\frac{d\omega'}{2\pi} - X_1\frac{i\Gamma_c\rho_\pm^{(0)}}{(\omega - 2\omega_L + i\gamma_2)(\omega + i2\Gamma)}\int_{-\infty}^{+\infty}\frac{\chi_1^*(\omega' - \omega)\chi_1(\omega')}{\omega' - \Delta_1 \pm \omega_L + i\Gamma}\frac{d\omega'}{2\pi}, \tag{58}$$

where $\Delta_1 \equiv \epsilon_g - \Omega_1$ is the detuning, and $X_1 \equiv |dE_{1+}|^2 - |dE_{1-}|^2$ is the circular degree of the pulse polarization. In the equation above, the first two terms correspond to the Raman coherence generated by the pump excitation[28], and the last two terms represent the spontaneously generated coherence. Obviously, for a linearly polarized pump, $X_1 = 0$, no spin coherence is generated either by excitation or by recombination, so there will be no spin beats in DTS.

In the short-pulse limit, the spin coherence after the pump and recombination can be approximately expressed as

$$\rho_{+,-}^{(2)}(t) \approx X_1|\chi_1(\Delta_1)|^2\left(\frac{\Gamma_c}{2\Gamma - \gamma_2 - 2i\omega_L} - \frac{1}{2}\right)e^{-i(2\omega_L - i\gamma_2)(t - t_1)}. \tag{59}$$

This formula can be directly compared to the result obtained by the intuitive picture in Sec. VI A. The physical meaning
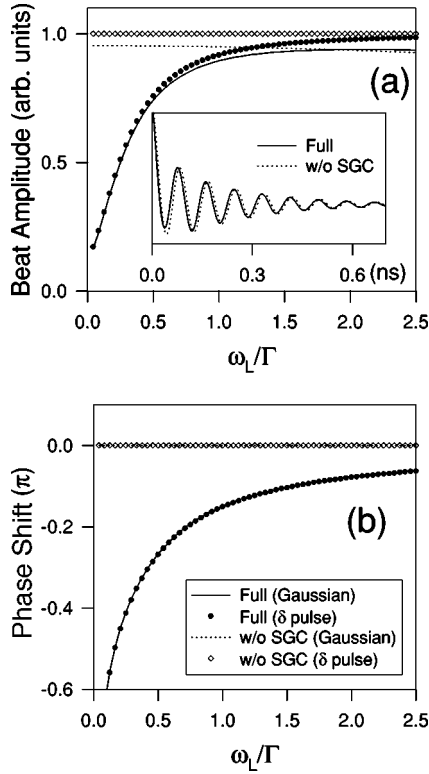
FIG. 3. (a) The amplitude and (b) the phase shift of the spin beat (shown in the insert) as functions of the Zeeman splitting in units of the trion state width, Γ. The filled circle and solid lines include the SGC effect, calculated with and without the short-pulse approximation, respectively. The diamond and dotted lines are the results without the SGC effect, calculated with and without the short-pulse approximation, respectively.

of the two terms in Eq. (59) is transparent: The first term is SGC, whose amplitude and phase shift depend on the ratio of the recombination rate to the Zeeman splitting, and the second term is just the optically pumped Raman coherence which in the short pulse limit is independent of the Zeeman splitting.

Having obtained the second-order results, we can readily derive the third-order density matrix and, in turn, the DTS can be calculated by use of Eq. (54). In general, the DTS can be expressed as

$$\Delta T \propto A \cos(2\omega_L t_d - \phi) e^{-\gamma_2 t_d} + B e^{-2\Gamma t_d} + C e^{-\gamma_1 t_d}, \quad (60)$$

and the spin coherence amplitude A and phase shift ϕ, the Pauli blocking amplitude B, and the spin nonequilibrium population C can all be numerically calculated and, in the short-pulse limit, can also be analytically derived as

$$A \approx |\chi_1(\Delta_1)|^2 |\chi_2(\Delta_2)|^2 X_1 X_2 \sqrt{\frac{\gamma_2^2 + 4\omega_L^2}{(2\Gamma_c - \gamma_2)^2 + 4\omega_L^2}}, \quad (61)$$

$$\phi \approx -\arctan\left(\frac{2\Gamma_c - \gamma_2}{2\omega_L}\right) - \arctan\left(\frac{\gamma_2}{2\omega_L}\right), \quad (62)$$

$$B \approx |\chi_1(\Delta_1)|^2 |\chi_2(\Delta_2)|^2 \left[I_1 I_2 + 2I_{1+}I_{2+} + 2I_{1-}I_{2-} \right.$$
$$\left. + X_1 X_2 \frac{2\Gamma_c(2\Gamma - \gamma_2)}{(2\Gamma - \gamma_2)^2 + 4\omega_L^2} \right], \quad (63)$$

$$C \approx 0, \quad (64)$$

where $\Delta_2 \equiv \epsilon_g - \Omega_2$ is the detuning, $I_{j\pm} \equiv |dE_{j\pm}|^2$, $I_j \equiv I_{j+} + I_{j-}$, and $X_j \equiv I_{j+} - I_{j-}$ ($j=1$ or 2). Thus, the short-pulse approximation yields expressions identical to the ones obtained from the intuitive picture in Sect. VI A. Several conclusions can be immediately drawn from the short-pulse approximation: (1) The SCP and OCP signals reveal beats with the same amplitude and opposite signs; (2) no spin beat can be observed when either of the pulses is linearly polarized ($X_1 = 0$ or $X_2 = 0$); and (3) due to the SGC effect, the beat amplitude increases with increasing Zeeman splitting until it saturates at the value it would have in the absence of the SGC effect; the phase shift increases from $-\pi/2$, saturating at 0. The SGC effect is negligible when the Zeeman splitting is large compared to the trion decay rate Γ because the rapid oscillation averages the effect of SGC to zero.

D. Numerical results

In the numerical simulations, we take the pump and the probe envelopes to be Gaussian $\chi_1(t) = \exp(-\eta_1^2 t^2/2)$ and $\chi_2(t - t_d) = \exp(-\eta_2^2(t - t_d)^2/2)$, and we assume that they have no temporal overlap, i.e., the delay time t_d is much larger than the pulse duration η_j^{-1} ($j=1,2$), and the pulse bandwidth η_j is greater than the relaxation rates γ_1, γ_2, and Γ. All these assumptions are well satisfied in the experiment.[13] Taken from the experiment,[13] the relaxation rates used are $\gamma_1 = 0$, $\gamma_2 = 3 \mu$eV, and $\Gamma = \Gamma_c = 12 \mu$eV, and $\eta_1 = \eta_2 = 0.5$ meV.

To minimize the effect of the background noise,[13] the measured data of DTS are presented as the difference between the SCP and OCP. We follow the same practice in presenting the theoretical results in Fig. 3. In comparison with the results without the SGC effect (dashed line), the full theoretical results show the phase shift of the spin beat in the DTS.

In Fig. 3, the amplitude and the phase shift are plotted against the Zeeman splitting $2\omega_L$, which is proportional to the magnetic field. The SGC effect is evident through the field dependence of the amplitude and phase shift of the spin beat. When the SGC effect is artificially switched off (by setting $\Gamma_c = 0$), the beat is independent of the magnetic field strength as long as the pulse spectrum is much broader than the Zeeman splitting. In the weak magnetic field limit, the spin coherence is strongly suppressed due to the destructive interference between the conventional Raman coherence and SGC; the phase shift then is about $-\pi/2$. In the strong magnetic field limit, as SGC is averaged to zero due to the rapid Larmor precession, the beat features approach those calculated without SGC. The theoretical predictions of the SGC effect on the pump-probe signals are in good agreement with the experimental results.[13]

VII. CONCLUSIONS

In this work, we have developed a theory to unite the different effects emerging from the spontaneous emission of a photon from a Λ system. We have taken the viewpoint that spontaneous emission is a unitary process when a sufficiently large quantum system is defined so as to be considered closed. Then the final state of the whole system, which is a pure state, can be projected in different ways. These projections can be thought of as measurements on one of the constituent parts and give rise to different phenomena: entanglement, spontaneously generated coherence, and two-pathway decay. We have also presented a set of conditions on the symmetry of a system which determine if there is SGC. Examples of specific atomic and solid-state systems have been employed to illustrate our theory. We have sketched the theory underlying the experiment in which SGC was observed[13] and we have proposed an experiment on the same system to exhibit the entanglement between the electron spin and the polarization of the spontaneously emitted photon in a quantum dot in parallel to the atom case.[8]

ACKNOWLEDGMENTS

[1] S. E. Harris, J. E. Field, and A. Imamoğlu, Phys. Rev. Lett. **64**, 1107 (1990).

[2] S. E. Harris, Phys. Rev. Lett. **62**, 1033 (1989).

[3] A. Imamoğlu, D. D. Awschalom, G. Burkard, D. P. DiVincenzo, D. Loss, M. Sherwin, and A. Small, Phys. Rev. Lett. **83**, 4204 (1999).

[4] A. Shabaev, Al. L. Efros, D. Gammon, and I. A. Merkulov, Phys. Rev. B **68**, 201305(R) (2003); P. Chen, C. Piermarocchi, L. J. Sham, D. Gammon, and D. G. Steel, *ibid.* **69**, 075320 (2004).

[5] C. Monroe, D. M. Meekhof, B. E. King, W. M. Itano, and D. J. Wineland, Phys. Rev. Lett. **75**, 4714 (1995).

[6] G. K. Brennen, C. M. Caves, P. S. Jessen, and I. H. Deutsch, Phys. Rev. Lett. **82**, 1060 (1999).

[7] R. B. Liu, W. Yao, and L. J. Sham, cond-mat/0408148 (unpublished).

[8] B. B. Blinov, D. L. Moehring, L.-M. Duan, and C. Monroe, Nature (London) **428**, 153 (2004).

[9] C. Cohen-Tannoudji, J. Dupont-Roc, and G. Grynberg, *Atom-Photon Interactions* (Wiley, New York, 1992).

[10] D. A. Cardimona and C. R. Stroud, Jr., Phys. Rev. A **27**, 2456 (1983).

[11] J. Javanainen, Europhys. Lett. **17**, 407 (1992).

[12] M. O. Scully and M. S. Zubairy, *Quantum Optics* (Cambridge University Press, Cambridge, UK, 1997).

[13] M. V. G. Dutt *et al.* (unpublished).

[14] V. Weisskopf and E. Wigner, Z. Phys. **63**, 54 (1930).

[15] C. H. Bennett, D. P. DiVincenzo, J. A. Smolin, and W. K. Wootters, Phys. Rev. A **54**, 3824 (1996).

[16] W. K. Wootters, Phys. Rev. Lett. **80**, 2245 (1998).

[17] M. B. Plenio, S. F. Huelga, A. Beige, and P. L. Knight, Phys. Rev. A **59**, 2468 (1999).

[18] X.-L. Feng, Z.-M. Zhang, X.-D. Li, S.-Q. Gong, and Z.-Z. Xu, Phys. Rev. Lett. **90**, 217902 (2003).

[19] Y.-H. Kim, R. Yu, S. P. Kulik, Y. Shih, and M. O. Scully, Phys. Rev. Lett. **84**, 1 (2000).

[20] K. W. Chan, C. K. Law, and J. H. Eberly, Phys. Rev. Lett. **88**, 100402 (2002).

[21] R. I. Dzhioev, V. L. Korenev, B. P. Zakharchenya, D. Gammon, A. S. Bracker, J. G. Tischler, and D. S. Katzer, Phys. Rev. B **66**, 153409 (2002).

[22] J. G. Tischler, A. S. Bracker, D. Gammon, and D. Park, Phys. Rev. B **66**, 081310(R) (2002).

[23] A. A. Kiselev, K. W. Kim, and E. Yablonovitch, Phys. Rev. B **64**, 125303 (2001).

[24] N. H. Bonadeo, J. Erland, D. Gammon, D. Park, D. S. Katzer, and D. G. Steel, Science **282**, 1473 (1998).

[25] W. Yao, R. B. Liu, and L. J. Sham, quant-ph/0407060 (unpublished).

[26] F. Bloch, Phys. Rev. **70**, 460 (1946).

[27] R. P. Feynman, F. L. Vernon, Jr., and R. W. Hellwart, J. Appl. Phys. **28**, 49 (1957).

[28] R. Leonhardt, W. Holzapfel, W. Zinth, and W. Kaiser, Chem. Phys. Lett. **133**, 373 (1987).

[29] N. Bloembergen, *Nonlinear Optics* (World Scientific, Singapore, 1996).

Stimulated and Spontaneous Optical Generation of Electron Spin Coherence in Charged GaAs Quantum Dots

M. V. Gurudev Dutt,[1] Jun Cheng,[1] Bo Li,[1] Xiaodong Xu,[1] Xiaoqin Li,[1] P. R. Berman,[1] D. G. Steel,[1,*] A. S. Bracker,[2]
D. Gammon,[2] Sophia E. Economou,[3] Ren-Bao Liu,[3] and L. J. Sham[3]

[1]*The H. M. Randall Laboratory of Physics, The University of Michigan, Ann Arbor, Michigan 48109, USA*
[2]*The Naval Research Laboratory, Washington, District of Columbia 20375, USA*
[3]*Department of Physics, The University of California-San Diego, La Jolla, California 92093, USA*
(Received 3 August 2004; published 9 June 2005)

We report on the coherent optical excitation of electron spin polarization in the ground state of charged GaAs quantum dots via an intermediate charged exciton (trion) state. Coherent optical fields are used for the creation and detection of the Raman spin coherence between the spin ground states of the charged quantum dot. The measured spin decoherence time, which is likely limited by the nature of the spin ensemble, approaches 10 ns at zero field. We also show that the Raman spin coherence in the quantum beats is caused not only by the usual stimulated Raman interaction but also by simultaneous spontaneous radiative decay of either excited trion state to a coherent combination of the two spin states.

The physics of quasizero dimensional semiconductor nanostructures or quantum dots (QDs) [1], and semiconductor electron spins, has been extensively investigated for developments in both basic science and technology [2]. The weak interaction of the electron spin in a QD with the environment is believed to lead to a long spin decoherence time $(T_2 \sim 1\text{--}100~\mu s)$ [3,4]. Recent measurements in GaAs and In(Ga)As QDs have also shown long spin relaxation times $(T_1 \sim 1\text{--}20~\text{ms})$ [5], which ultimately limits T_2. However, coherent preparation and detection of the spin states is a challenge remaining to be addressed, with recent work in silicon devices demonstrating the rapid progress being made in this area [6].

In this Letter, we report on the coherent optical generation of electron spin polarization in the ground state of charged GaAs QDs via resonant excitation of an intermediate charged exciton (trion) state. Stimulated Raman excitation by coherent optical pulses of the Raman coherence between the spin ground states of the QD is thus demonstrated. The results will further show that the spin decoherence time is $\sim$10 nsec at zero field and that there are two contributions to the spin coherence: an induced part arising from coherent optical coupling of the spin states through stimulated Raman excitation, and a *spontaneously generated coherence* (SGC) arising from radiative decay of the trion into the spin states.

In the absence of magnetic fields, the Zeeman sublevels of the electron in the conduction-band ground state of a charged QD are assumed degenerate. The lowest optically excited state is a trion state consisting of a singlet pair of electrons and a heavy hole with its spin pointing up or down along the growth axis, designated as the z axis. The application of a magnetic field in the Voigt geometry [$\theta = 0°$ in Fig. 1(a)] leads to the excitation level scheme shown in Fig. 1(b) [7]. This scheme is equivalent to the three-level Λ systems used in demonstration of various quantum-

optical phenomena, such as electromagnetically induced transparency [8], lasing without inversion [9], and slowing and freezing of light [10], which rely on the existence of a ground state Raman coherence [11].

The physical origin of the stimulated Raman coherence can be understood in terms of the optical orientation of the spin in the growth (light propagation) direction. The spin states quantized in the z direction are superpositions of the spin states quantized in the magnetic field direction $[|z\pm\rangle \equiv (|x+\rangle \pm |x-\rangle)/\sqrt{2}]$, and thus the spin vector oriented along the z direction represents coherence between the spin eigenstates $|x\pm\rangle$ in the magnetic field. For simplicity, we assume that before the application of the pump pulse, the system is unpolarized. In the short-pulse limit, the σ^- pulse excites only the spin down state $|z-\rangle$ to the trion state $|t-\rangle$, leaving the electron polarized in the spin up z direction. In the transverse magnetic field,
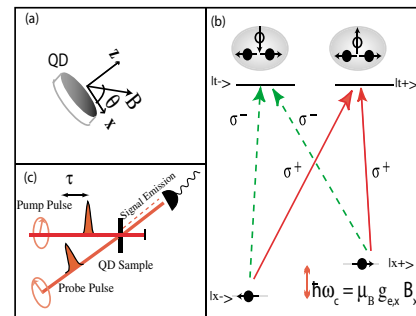

FIG. 1 (color online). (a) Magnetic field (**B**) orientation with respect to QD. (b) Excitation picture for the charged QD in the Voigt geometry ($\theta = 0°$), with ground states $|x\pm\rangle$ denoting electron spin projections $\pm\frac{1}{2}$ along the x axis split by $\hbar\omega_c$. The trion states $|t\pm\rangle$ are labeled by the heavy-hole angular momentum projection $\pm\frac{3}{2}$ along the z axis. Solid (dashed) lines denote transitions excited by σ^+ (σ^-) light. (c) Schematic of DT experimental setup.

the induced spin polarization (or Raman coherence) precesses and thus the optically generated population of the spin state $|z-\rangle$ oscillates as

$$\rho_{z-,z-}^{R}(\tau) = -\rho_{t-,t-}\frac{1 + e^{-\gamma_s \tau}\cos(\omega_c \tau - \phi)}{2}, \quad (1)$$

where $\rho_{t-,t-}$, proportional to the intensity of the pump pulse, denotes the population of the trion state immediately after the pump pulse, and ω_c, γ_s are the Larmor frequency and spin decoherence rate, respectively. For the case of stimulated Raman quantum beats (QBs) given by Eq. (1), the phase $\phi = 0$.

The stimulated Raman processes which yield the QBs in Eq. (1) can also be illustrated with a perturbation sequence using the density matrix operator ρ for the four-level scheme shown in Fig. 1. The pump pulse ($\mathbf{E_1}(t)$) coherently excites the Raman coherence ($\rho_{x+,x-}$) to second order in the field, and the probe pulse ($\mathbf{E_2}(t - \tau)$) converts this to a nonlinear polarization ($\propto \rho_{t-,x-}$) which copropagates with the probe field [12],

$$\rho_{x-,x-} \xrightarrow{\mathbf{E_1}(\sigma^-)} \rho_{t-,x-} \xrightarrow{\mathbf{E_1^*}(\sigma^-)} \rho_{x+,x-} \xrightarrow{\mathbf{E_2}(\sigma^+)} \begin{cases} \rho_{t-,x-} \\ \rho_{t+,x-} \end{cases}.$$

The two upper levels are necessary in order to correctly account for the polarization dependence, but the QBs are present in the three-level Λ system. Within the sample, the four-wave mixing (FWM) signal field arises from the third order nonlinear optical polarization [Fig. 1(c)]. The differential transmission (DT) signal represents the homodyne detection of the FWM response propagating collinearly with the reference probe field [13–15]. In our experiments, the pump and probe laser fields can have either parallel (PCP) or orthogonal circular polarization (OCP), and the DT signal was obtained using balanced phase-sensitive detection.

The above picture of spin QBs arising from stimulated excitation of the Raman coherence has been extremely successful [14–18]. However, it has also been anticipated that the spontaneous emission from the trion state can result in a coherent combination of the two spin states, known as spontaneously generated coherence (SGC) [19,20]. Spontaneous emission is commonly considered to destroy coherence, but when (i) the Zeeman splitting $\hbar\omega_c$ is comparable to or smaller than the trion decay rate $2\Gamma_t$, and (ii) the transition dipole moments from the trion state to the two spin states are nonorthogonal, different transitions can couple to the same modes of the electromagnetic vacuum. For instance, the transitions between $|t-\rangle$ and $|x\pm\rangle$ can couple to the same vacuum mode with polarization σ^-, thus creating coherence between the final states ($|x\pm\rangle$) of the spontaneous emission process. In the optical orientation picture, the trion state $|t-\rangle$ will relax back to the state $|z-\rangle$ by spontaneously emitting a σ^- polarized photon, thus giving rise to coherence between the energy eigenstates $|x+\rangle$ and $|x-\rangle$. Although there have been numerous theoretical studies

previously [19,20], there had been no experimental observation of an excited-state population decaying to a ground state Raman coherence. From the detailed analysis to be presented later, a portion of the Raman coherence caused by SGC is $\pi/2$ out of phase and interferes destructively with the stimulated Raman coherence, giving rise to a nonzero phase ϕ in Eq. (1).

For our work, the sample consisted of interface fluctuation GaAs QDs, formed by growth interrupts at the interface of a narrow (4.2 nm) GaAs quantum well, which were remotely doped with electrons. Magneto-photoluminescence measurements on single charged QDs showed a small electron g factor [21] that implies a maximum splitting $\hbar\omega_c \sim 80\ \mu eV$ at the highest fields reached in our experiments. The etched sample was mounted in a superconducting magnetic cryostat held at 4.8 K. The pump and probe pulses were obtained from a mode-locked Ti:Sapphire laser, with a shaped pulse bandwidth (FWHM = 0.84 meV) that exceeds the splitting between the electron spin states.

Figure 2(a) shows the nonlinear optical spectrum with two peaks corresponding to trions (T) and excitons (X) trapped in charged and neutral QDs, respectively [21]. In Fig. 2(c) [2(d)] we plot the difference between DT signal obtained for the PCP and OCP configurations, with the laser tuned to resonantly excite neutral [charged] QDs at X [T]. The data in Fig. 2(d) was fitted using the equation,

$$\mathrm{DT}_{\mathrm{PCP-OCP}} = A_1 e^{-2\Gamma_t \tau} + A_2 e^{-\gamma_s \tau}\cos(\omega_c \tau - \phi) \quad (2)$$
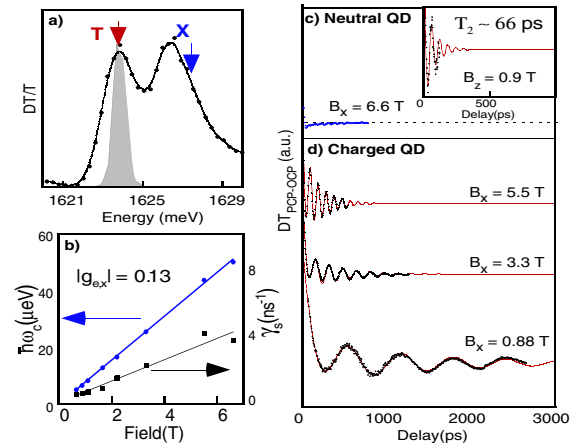

FIG. 2 (color online). (a) DT spectrum with the pulse delay fixed at +10 ps. The shaded region is the pulse spectrum, and the arrows at T (X) label the trion (exciton) resonances. (b) Variation of the decay rate and the oscillation frequency with the field. We extract the g factor to be $|g_{e,x}| = 0.13$. (c) DT signal at X for $B_x = 6.6$ T showing no oscillations. Inset: Single QD exciton QBs obtained in the Faraday geometry with $B_z = 0.9$ T [16]. (d) Spin QBs in DT signal as a function of in-plane magnetic field B_x, obtained when the laser pulse is tuned to selectively excite the T resonance. Data shown in (c) and (d) are the differences between PCP and OCP signals. Solid lines show fits to the data using Eq. (2).

which was obtained from the theory [22], and the resulting values for $\hbar\omega_c$ and γ_s are plotted in Fig. 2(b) as a function of the field. The oscillation frequency (ω_c) depends on the splitting between the states and allows us to find $|g_{e,x}| = 0.13$ in good agreement with [21]. The theory shows that the first term in Eq. (2) arises from the incoherent contribution due to the Pauli blocking effect, and decays with the trion recombination rate $2\Gamma_t \sim (84 \text{ ps})^{-1}$. The second term, describing the beats, arises from the coherent contribution ($\rho_{x+,x-}$) or the net precessing spin polarization in the z direction, and decays with the spin decoherence rate γ_s. Hole spin relaxation between the two trion states was accounted for and affects the Pauli blocking term only, but not the QBs.

The spin dephasing time $T_2^*(= 1/\gamma_s) \sim 10$ ns was obtained from the zero-field intercept in Fig. 2(b), which is much smaller than the T_2 predicted by theory [3,4]. Electrons in different dots or in the same dot at different times experience different random orientations of the hyperfine nuclear fields. If in each dot the electron interacts with $N \sim 10^6$ nuclei, the characteristic timescale due to the spatial fluctuations in the hyperfine interaction is $T_N \approx \hbar\sqrt{N}/A = 6$ ns [3], where $A \approx 90$ μeV is the hyperfine constant for GaAs, comparable to the decay times obtained here. Our ensemble measurements are consistent with a previous Hanle study of a single dot in the same system [23]. The linear change in γ_s with the magnetic field is commonly attributed to a Gaussian distribution of g factors [18], from which we obtain a width $\Delta g/g \sim 8\%$.

In contrast to the T resonance, tuning the laser to the X resonance results in vanishing of the beats as seen in Fig. 2(c). As discussed in Refs. [15–17], the exciton behaves as a three-level V system. The fast exciton recombination time (~ 50–100 ps [24]) and the small Zeeman splitting in the Voigt geometry results in overdamping of the exciton Raman coherence. For comparison, the inset to Fig. 2(c) shows DT QBs of magneto-excitons in a single neutral QD obtained in the Faraday geometry ($\theta = 90°$), where the splitting is enhanced by the large g factor.
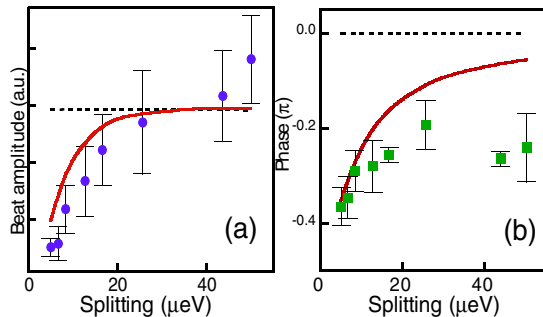

FIG. 3 (color online). (a) and (b) show the changes in the amplitude (A_2) and phase (ϕ) of the oscillations as a function of splitting. Solid (dashed) lines denote theoretical predictions for these parameters with (without) the effects of SGC. In numerical calculations, the optical pulses are assumed Gaussian, i.e., $I(\omega) = \exp(-\omega^2/2\sigma^2)$ ($\sigma = 0.35$ meV).

Reference [16] reports that the exciton Raman decoherence time ($T_2 \sim 66$ ps) is limited by recombination.

When there are no effects due to SGC, and in the limit where the pulse bandwidth is much greater than the Zeeman splitting, the amplitude and phase shift of the spin Raman coherence generated by the pump pulse should be independent of the Zeeman splitting. This is verified by the theory, as shown in the dashed lines of Fig. 3. However, the data (solid symbols) in Figs. 3(a) and 3(b) demonstrates a clear dependence of the beat amplitude (A_2) and phase (ϕ) on the Zeeman splitting $\hbar\omega_c$ which has not been reported in earlier experiments [14–18]. We verified that the dependence is not due to shifts in the trion resonance, or changes in the oscillator strength with magnetic field. As elaborated below, the data in Fig. 3 provides experimental confirmation for SGC.

Specifically, the spin polarization or coherence spontaneously generated in the time interval ($t, t + dt$) for $t < \tau$ after the pump pulse can be determined by the population generated in $|z-\rangle$ [22,25],

$$d\rho_{z-,z-}^{\text{SGC}} = \Gamma_t\rho_{t-,t-}e^{-2\Gamma_t t}\{1 + e^{-\gamma_s(\tau-t)}\cos[\omega_c(\tau-t)]\}dt.$$
$$(3)$$

Thus, the spin coherence accumulated from $t = 0$ to $t = \tau$ via the trion recombination process is dependent on the Zeeman splitting. Combining the contributions from the pump-excited Raman coherence in Eq. (1) and from SGC yields spin beats with amplitude and phase shift given, in the short-pulse limit, by

$$A_2 \approx \sqrt{\frac{\gamma_s^2 + \omega_c^2}{(2\Gamma_t - \gamma_s)^2 + \omega_c^2}},$$
$$(4)$$

$$\phi \approx -\arctan\left(\frac{2\Gamma_t - \gamma_s}{\omega_c}\right) - \arctan\left(\frac{\gamma_s}{\omega_c}\right).$$
$$(5)$$

In the weak magnetic field limit, the trion decay is much faster than the spin precession, and so the SGC cancels the conventional Raman coherence. In the strong magnetic field limit, the rapid spin precession averages the SGC to zero. This explains the observed field dependence of the spin beats in Fig. 3. As the Zeeman splitting increases from zero to much larger than the radiative decay rate, the beat amplitude increases until it saturates at the value calculated without the SGC effect, and the phase shift increases from close to $-\pi/2$ to zero.

In the master equation for the Λ system, derived in the Markov-Born approximation, the SGC effect appears as

$$\dot{\rho}_{x+,x-}|_{\text{SGC}} = -\Gamma_t\rho_{t-,t-}.$$
$$(6)$$

A full numerical solution of the master equation, taking into account the finite pulse width, is performed at each magnetic field value for the time delay dependence of the DT signal, with the input parameters taken from experiment for the Zeeman splitting, spin dephasing rate, and trion decay rate [22]. Thus, the amplitude and phase of the

spin beats computed as a function of the Zeeman splitting are shown as solid lines in Fig. 3, similar to the results obtained in the short-pulse limit. The agreement of the SGC theory with experimental data is good. The deviation of the theory and experiment as a function of magnetic field compared to the expected behavior in the absence of SGC is evident.

Physically, as discussed above, the same mode of the vacuum field simultaneously couples the trion state to the two spin states and gives rise to SGC in our experiments. In atomic systems, ground state Raman coherence induced by population decay from an excited state has been difficult to observe due to the conditions (i) and (ii) that must be simultaneously met. However, recently an entangled state between a single ion and two modes of the radiation field was observed [26], an effect which can be interpreted as complementary to SGC [22]. The observation of SGC in QDs is favored not only by the relatively large radiative decay rate as compared to the spin precession rate, but also by the ability to tailor the quantum states in the artificial atoms by magnetic field and by doping.

The results of this work bear directly on proposals for using optically driven charged QDs for quantum computing (QC) [7,27]. In this regard, significant progress has already been made in demonstrating many of the key DiVincenzo requirements for QC [28] with excitonic optical Bloch vector qubits in neutral QDs, such as single qubit rotations [29], quantum entanglement [30], and conditional quantum logic gates [31]. These results illustrate the close analogy between artificial atoms and QDs [1], but the short decoherence time of the exciton (0.1–1 ns [24,32]) constrains quantum error correction schemes. In the present work, we have demonstrated that a coherent optical field can create a coherent superposition of electron spin states in QDs. While the measured decoherence time has a limiting value of 10 ns, much longer than the exciton decoherence time, the lifetime is shorter than anticipated due to ensemble averaging, as discussed previously. Coherent spectroscopy measurements on a single dot could eliminate some aspects of this averaging. Single qubit rotations are a logical next step remaining to be pursued, for example, through off-resonant Raman processes as proposed in Ref. [33]. Modifications to the selection rules, caused by the small heavy-light-hole mixing (~ 0.06), will merely result in slight changes to the axis and angle of the Raman induced spin qubit rotation, which can be compensated optically.

---

*Electronic address: dst@umich.edu

[1] A. D. Yoffe, Adv. Phys. **50**, 1 (2001); P. M. Petroff, A. Lorke, and A. Imamoğlu, Phys. Today **54**, 5, 46 (2001); D. Gammon and D. G. Steel, Phys. Today **55**, 10, 36 (2002); E. Beham *et al.*, Phys. Status Solidi C **1**, 2131 (2004).

[2] S. A. Wolf *et al.*, Science **294**, 1488 (2001); A. Zutic, J. Fabian, and S. D. Sarma, Rev. Mod. Phys. **76**, 323 (2004).

[3] A. V. Khaetskii, D. Loss, and L. Glazman, Phys. Rev. Lett. **88**, 186802 (2002); I. A. Merkulov, A. L. Efros, and M. Rosen, Phys. Rev. B **65**, 205309 (2002).

[4] R. de Sousa and S. Das Sarma, Phys. Rev. B **67**, 033301 (2003).

[5] J. M. Elzerman *et al.*, Nature (London) **430**, 431 (2004); M. Kroutvar *et al.*, *ibid.* **432**, 81 (2004).

[6] D. Rugar *et al.*, Nature (London) **430**, 329 (2004); M. Xiao *et al.*, *ibid.* **430**, 435 (2004).

[7] A. Imamoğlu, Fortschr. Phys. **48**, 987 (2000).

[8] K. J. Boller, A. Imamoğlu, and S. E. Harris, Phys. Rev. Lett. **66**, 2593 (1991).

[9] S. E. Harris, Phys. Rev. Lett. **62**, 1033 (1989); M. O. Scully, S. Y. Zhu, and A. Gavrielides, *ibid.* **62**, 2813 (1989).

[10] L. V. Hau *et al.*, Nature (London) **397**, 594 (1999); C. Liu *et al.*, *ibid.* **409**, 490 (2001).

[11] M. Lindberg and R. Binder, Phys. Rev. Lett. **75**, 1403 (1995).

[12] I. M. Beterov and V. P. Chebotaev, Prog. Quantum Electron. **3**, 1 (1974).

[13] In the absence of mutual pump/probe coherence, DT is simply the difference between the probe absorption with and without the pump excitation. See also Refs. [14,15].

[14] K. B. Ferrio and D. G. Steel, Phys. Rev. Lett. **80**, 786 (1998).

[15] A. S. Lenihan *et al.*, Phys. Rev. Lett. **88**, 223601 (2002).

[16] Xiaoqin Li *et al.*, Phys. Rev. B **70**, 195330 (2004).

[17] A. I. Tartakovskii *et al.*, Phys. Rev. Lett. **93**, 057401 (2004).

[18] J. A. Gupta *et al.*, Phys. Rev. B **59**, R10421 (1999).

[19] J. Javanainen, Europhys. Lett. **17**, 407 (1992); G. C. Hegerfeldt and M. B. Plenio, Phys. Rev. A **46**, 373 (1992); S. Menon and G. S. Agarwal, *ibid.* **57**, 4014 (1998).

[20] S. Y. Zhu, and M. O. Scully, Phys. Rev. Lett. **76**, 388 (1996); P. R. Berman, Phys. Rev. A **58**, 4886 (1998).

[21] J. G. Tischler *et al.*, Phys. Rev. B **66**, 081310 (2002).

[22] S. E. Economou *et al.*, Phys. Rev. B **71**, 195327 (2005).

[23] A. S. Bracker *et al.*, Phys. Rev. Lett. **94**, 047402 (2005).

[24] N. H. Bonadeo *et al.*, Phys. Rev. Lett. **81**, 2759 (1998).

[25] A. Shabaev *et al.*, Phys. Rev. B **68**, 201305 (2003).

[26] B. B. Blinov *et al.*, Nature (London) **428**, 153 (2004).

[27] C. Piermarocchi *et al.*, Phys. Rev. Lett. **89**, 167402 (2002); F. Troiani, E. Molinari, and U. Hohenester, *ibid.* **90**, 206802 (2003); E. Pazy *et al.*, Europhys. Lett. **62**, 175 (2003); T. Calarco *et al.*, Phys. Rev. A **68**, 012310 (2003).

[28] D. P. DiVincenzo, Fortschr. Phys. **48**, 771 (2000).

[29] T. H. Stievater *et al.*, Phys. Rev. Lett. **87**, 133603 (2001); H. Kamada *et al.*, *ibid.* **87**, 246401 (2001); H. Htoon *et al.*, *ibid.* **88**, 087401 (2002); A. Zrenner *et al.*, Nature (London) **418**, 612 (2002).

[30] Gang Chen *et al.*, Science **289**, 1906 (2000).

[31] Xiaoqin Li *et al.*, Science **301**, 809 (2003).

[32] P. Borri *et al.*, Phys. Rev. Lett. **87**, 157401 (2001).

[33] P. Chen *et al.*, Phys. Rev. B **69**, 075320 (2004).

Theory of spontaneously generated spin coherence in nanodots

Sophia Economou, Renbao Liu and L. J. Sham

Department of Physics, University of California San Diego, La Jolla, California 92093-0319

Phone: (858) 822-1018 Fax: (858) 534-2232 Email: economou@physics.ucsd.edu

Abstract: Spontaneously generated spin coherence was recently established experimentally for a Λ-system in a semiconductor nanodot. The theory underlying the experiment is sketched and an intuitive picture based on the spin vector model is given.

©2004 Optical Society of America

OCIS codes: (300.6240) Coherent transient spectroscopy; (300.6470) Semiconductor Spectroscopy; (270.1670) Coherent optical effects

The two electron spin states in a doped semiconductor nanodot have been proposed as a solid-state qubit [1]. An optical scheme for the quantum operations involves an intermediate trion state, which constitutes the excited state of a Λ scheme [2]. The two spin states are split by a static in-plane magnetic field, and the pulse used is circularly polarized along the growth direction, and tuned close to the trion state composed of two electrons in the singlet state and a heavy hole. Due to the small in-plane g factor of the heavy hole, the trion state is rather insensitive to magnetic fields up to 5T [3]. The principal decay mechanism for the trion state is radiative recombination of the one electron with the hole. The polarization selection rules for this system are such that the trion will relax to a linear combination of the two spin states, which is another spin state, polarized along the growth direction. This is an example of spontaneously generated coherence (SGC). For this effect to be detectable, the splitting between the two lower levels has to be small compared to the linewidth of the trion state. This requirement is feasible in the trion system, since by controlling the magnetic field we can tune the splitting.

In a pump-probe experiment on this system, quantum spin beats are seen in the probe signal. The beats have two contributions: one from the coherence induced by the pump laser (Raman coherence), and one from SGC, as explained above. To calculate the nonlinear response, an order-to-order calculation may be carried out. We have used this perturbative method to calculate the probe response when the SGC term is included, and we have found a dependence of the amplitude and the phase shift of the signal on the static magnetic field. In the absence of SGC there is no dependence of these quantities on the field strength . Our results are in good agreement with the experiment [4].

To obtain an intuition on how this phase shift and amplitude dependence on the magnetic field occurs, we employ the vector model of the mean value of the spin. Initially, the system is in a spin ensemble, i.e. a completely mixed state. The pump pulse is polarized such that it connects only the $|z\rangle$ state to the trion state $|t\rangle$; the $|\bar{z}\rangle$ state is not dipole connected to $|t\rangle$, i.e. it is a dark state. When the pump excites the transition $|z\rangle \to |t\rangle$ there is an excess $|\bar{z}\rangle$ population. When rotated to the x basis, it amounts to coherence between the two s_x eigenstates; this is the Raman coherence. The spin vector, which is initially pointing along $-z$, precesses about the B-field (Larmor precession). This precession manifests itself as quantum beats. When SGC is also accounted for, and when the decay process is fast compared to the precession rate, soon after the spin vector starts to precess, one trion relaxes to $|z\rangle$ and a little vector along $+z$ adds to the spin vector. This process continues until all the trions have decayed. From a simple geometrical construction (Fig. 1) we can see that there is a phase shift and an amplitude difference between the cases with and without SGC. Note also that in the opposite limit, when the precession is fast, i.e. when the Zeeman splitting is large as compared to the trion state linewidth, the contributions along $+z$ add when the spin vector is in a random position, and so they average out.

According to the above discussion, SGC arises from the relaxation to a single state, which is not an energy eigenstate. If there was no B field, then any spin basis would comprise a good energy basis. In the system discussed here then, the s_z eigenstates would be special from a symmetry point of view, since z is the growth axis and the optical axis. We could therefore view an in-plane magnetic field as a breaking of this symmetry,
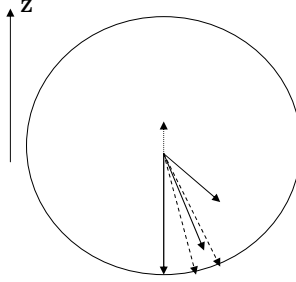
Fig. 1. Projection of the Bloch sphere. The solid arrow represents the spin vector at three different instants, as modified by SGC. The small dotted arrow is the contribution of SGC to the Bloch vector. The dashed arrow is the spin vector in the absence of SGC. The phase shift and the amplitude difference of the two vectors, measured in the pump-probe experiment, are clearly demonstrated in the geometrical picture.

which induces SGC. In this context, we have determined a set of conditions on the field contribution to the Hamiltonian, H^B, and on the separation between the lower levels, ϵ, for SGC to appear. In a system with an axial symmetry and optical selection rules determined by $\mathcal{J}_z$, a perturbation H^B will cause SGC to appear if the following conditions are satisfied:

(i) $[H^B, \mathcal{J}_z] \neq 0$;

(ii) $H^B|e\rangle \propto |e\rangle$;

(iii) $|\epsilon| \lesssim \Gamma$.

H^B may or may not be induced by an external field. In atoms, the role of H^B can be played by the spin-orbit coupling. However, the atomic states are long-lived and therefore SGC between states split by the spin-orbit interaction is not observable. The role of H^B can even be played by measurement, when control over the spontaneously emitted photon is possible.

References

[1] D. Loss and D.P. DiVincenzo, "Quantum Computation with Quantum Dots," Phys. Rev. A **57**, 120-126 (1998).

[2] P. Chen, C. Piermarocchi, L. J. Sham, D. Gammon, D. G. Steel, "Theory of Quantum Optical Control of Single Spin in Quantum Dot," Phys. Rev. B **69**, 075320 (2004).

[3] J. G. Tischler, A. S. Bracker, D. Gammon and D. Park, "Fine structure of trions and excitons in single GaAs quantum dots," Phys. Rev. B **66**, 081310 (2002).

[4] M. V. G. Dutt, J. Cheng, B. Li, X. Xu, X. Li, D. G. Steel, A. S. Bracker, D. Gammon, S. E. Economou, R. Liu, and L. J. Sham, submitted for publication.

Theory proposal of electron spin rotation in a quantum dot

Sophia Economou and L. J. Sham

Department of Physics, University of California San Diego, La Jolla, California 92093-0319
Phone: (858) 822-1018 Fax: (858) 534-2232 Email: economou@physics.ucsd.edu

Yanwen Wu and D. G. Steel

H. M. Randall Laboratory, The University of Michigan, Ann Arbor, MI 48109
Phone: (734) 764-4469 Fax: (734) 763-9694, Email: dst@eecs.umich.edu

Abstract: We propose an optical scheme to probabilistically initialize and rotate the electron spin in a quantum dot using charged exciton states. Our proposal makes use of the properties of the sech pulses for two-level systems.

The spin of an electron trapped in a quantum dot is a candidate for a quantum bit in quantum information processing proposals. The merits of manipulating the spin optically, by use of intermediate charged exciton states (trions), are the ready availability of the lasers and the fast operational times. The spin rotation is yet to be shown experimentally, and this will comprise an important step toward the implementation of this solid state proposal.

The two spin states of the doped electron and the intermediate trion form a three-level Λ type system. A static in-plane magnetic field is used to split the two spin states, and the pulses used are circularly polarized along the growth direction (z axis). The Zeeman splitting is on the order of tens of μeV's in GaAs [1], and the trion state is rather insensitive to magnetic fields up to 5T [2], so that the trion polarized along z does not rotate about the perpendicular B field. It is useful to view this three-level system in the z basis rather than in the energy eigenbasis; due to polarization selection rules, only the $|+z\rangle$ state couples to the trion. Moreover, for pulses fast compared to the spin precession, the $|-z\rangle$ state can be ignored in the qualitative discussion of the quantum evolution. The objective is a rotation of the spin via a unitary operation. The trion state is an auxiliary level in this process. Therefore, the control pulse should leave no population in the trion state; we will refer to such pulses as 'transitionless'. The effect of transitionless pulses is to give a phase to the $|+z\rangle$ state relative to the trion but also, and most importantly, relative to the $|-z\rangle$ state. A unitary operation causing a phase change ϕ between the two $|\pm z\rangle$ states is a rotation about the z axis by an angle ϕ. We also give an analytic expression for this angle as a function of the input, i.e., the laser parameters.

A well-known pulse shape in quantum optics is the *sech* pulse of Rosen and Zener [3], which is an exactly solvable pulse in the two-level system, for any detuning. In the interaction picture the coupling matrix element takes the form

$$V_{tz}(t) = \Omega \, \text{sech}(\sigma t) \, e^{i\Delta t}, \tag{1}$$

where Ω, σ and Δ are the Rabi frequency, the bandwidth and the detuning of the pulse respectively. In our quasi two-level system, formed by the $|+z\rangle$ state and the trion $|t\rangle$, the population of the trion state after the passage of the pulse is given by

$$\rho_{tt} = \rho_{zz}^0 \sin^2\left(\frac{\Omega}{\sigma}\pi\right) \text{sech}^2\left(\frac{\Delta}{2\sigma}\pi\right), \tag{2}$$

where ρ_{zz}^0 is the population of the $|+z\rangle$ state before the action of the pulse. The typical temperature for such experiments is 4K, which is well above the Zeeman splitting, and therefore the initial state of the system will be a thermal equilibrium of the two states, that is, $\rho_{zz}^0 = 1/2$. From Eq. (2) we see that we can achieve a 50% probability of initializing a spin along z with a single-shot pulse when $\Omega = \sigma/2$ and $\Delta = 0$, so that the
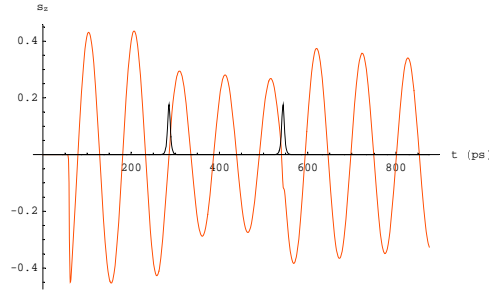
Fig. 1. The spin vector is generated by the pump and subsequently rotated via the control pulse, by an angle $\pi/4$ about z. A second control pulse rotates the spin vector back, restoring the amplitude of the beats, thus demonstrating the unitarity of the control. The control pulses are also shown.

Rosen-Zener pulses can also be used for initialization. For an actual quantum computation, we would need to repeat the pulse to increase the fidelity of the initialization, but for demonstration purposes this amount of spin polarization is sufficient. For a Zeeman splitting large compared to the trion linewidth, the radiative recombination of the trion will incoherently relax it to the lower spin states [1, 4], and we are thus left with a spin vector initially pointing along $|z\rangle$ and precessing in the yz plane. A second pulse, the control pulse, rotates the spin vector via the aforementioned mechanism. The control pulse should be transitionless, which translates to $\Omega = \sigma$ from Eq. (2). Then, the angle of rotation is given by

$$\phi = 2 \arctan\left(\frac{\sigma}{\Delta}\right). \tag{3}$$

From Eq. (3) it is evident that for a fixed pulse duration (fixed σ), variation of the detuning Δ will determine the angle of rotation. To demonstrate the unitarity of the control operation (no population transfer to the trion), a second control pulse should be used to rotate the spin vector back and restore the beats, as shown in Fig. .

The fidelity of the operation will deteriorate due to the following: first, the $|-z\rangle$ state actually precesses during the pulse action. However, this does not affect the unitarity of the operation, and it merely tilts by a small amount the axis of rotation; second, the trion state decays via spontaneous emission during the short time it gets populated by the control pulse, which suggests that short pulses should be used. There is however a limit to how short a pulse may be used, since the strength of the pulse will have to be simultaneously increased. Our numerical simulations show that there is a range in the parameter space where the operation is feasible, with fidelities higher than 99.6%.

One of the strengths of this proposal is its analyticity: for given input (σ and Δ), the output is determined (rotation angle ϕ about z). It is however only providing a recipe for rotations about z. The next step is to design and experimentally implement rotations about other axes.

References

[1] M. V. G. Dutt, J. Cheng, B. Li, X. Xu, X. Li, D. G. Steel, A. S. Bracker, D. Gammon, S. E. Economou, R. Liu, and L. J. Sham, "Stimulated and Spontaneous Optical Generation of Electron Spin Coherence in Charged GaAs Quantum Dots," Phys. Rev. Lett. **94**, 227403 (2005).

[2] J. G. Tischler, A. S. Bracker, D. Gammon and D. Park, "Fine structure of trions and excitons in single GaAs quantum dots," Phys. Rev. B **66**, 081310 (2002).

[3] N.Rosen and C. Zener, "Double Stern-Gerlach Experiment and Related Collision Phenomena," Phys. Rev. **40**, 502-507 (1932).

[4] Sophia E Economou, Ren-bao Liu, L. J. Sham, and D. G. Steel, "Unified theory of consequences of spontaneous emission in a Λ type system," Phys. Rev. B **71**, 195327 (2005).

Coherent ultrafast optically controlled rotation of electron spins in charged quantum dots

Yanwen Wu, Erik D. Kim, Jun Cheng, Xiaodong Xu, Qiong Huang, Hailing Cheng, and D. G. Steel

H. M. Randall Laboratory, The University of Michigan, Ann Arbor, MI 48109
Phone:(734) 764-4469 Fax: (734) 763-9694, Email: dst@eecs.umich.edu
http://www.physics.lsa.umich.edu/dst

D. Gammon

Naval Research Laboratory, Washington DC 20375
Phone: (202) 404-4533 Fax: (202) 767-1165, Email: gammon@nrl.navy.mil

Sophia Economou and L. J. Sham

Department of Physics, The University of California, San Diego
La Jolla, California 92093
Phone: (858) 534-3269 Fax: (858) 534-2232, Email: lsham@ucsd.edu

Abstract: We demonstrate coherent ultrafast optically controlled rotation of electron spins in an ensemble of charged quantum dots, laying the ground work for spin initialization and Rabi oscillations.
© 2005 Optical Society of America
OCIS codes: (300.6420)Coherent Transient Spectroscopy; (300.6470)Semiconductors Spectroscopy

The electron spin in semiconductor nanostructures is the subject of numerous studies because of its expected long spin coherence time ($\sim$1 ms) [1, 2, 3, 4] and its potential for implementation as an applicable qubit in quantum information processing [5]. Here we report an all optical coherent ultrafast manipulation of an ensemble of electron spin polarization in charged quantum dots (QDs), a crucial step towards spin initalization and spin Rabi oscillation and hence single qubit rotation in such system.

The QD's are formed by interface fluctuations in a 4.2 nm GaAs/Al$_{0.3}$Ga$_{0.7}$As layer which is modulation doped with silicon. The excess electrons from the silicon are trapped in the dot potential forming charged QD. The experiment is conducted in a magnetic field of B=6.6 T perpendicular ($\vec{x}$) to the growth direction ($\vec{z}$) (Voigt geometry) at 4K with a modulated pump and probe pair and an unmodulated control beam with pulse widths of 6 ps (0.4 meV). The frequency of all three beams are fixed at the ensemble trion transition. The data is taken by fixing the control delay (τ_c) to the pump at various positions and scanning the probe delay to map the dynamics of the system. The differential transmission (DT) signal is homodyne detected with the transmitted probe beam.

The energy levels in the charge QD are described by two electron spin ground states ($|x\pm\rangle$) quantized along $\vec{x}$ and two charged exciton (trion) states ($|t\pm\rangle$). By using one polarization of light, σ_- for example, we isolate a Λ system as seen in the dashed box in Fig. 1a. The splitting of the spin states is 49 μeV for B=6.6 T and the splitting of the trion states is 0 due to its negligible in-plane g-factor. At 4K, the thermal excitation energy is around 0.3 meV much greater than the splitting, which means the system is in thermal equilibrium with equal population in both spin states (i. e. no net polarization).

In order to control the spin polarization, we must first create a spin polarization in the system. The pump pulse to second order generates a net spin polarization along the optical axis $\vec{z}$. This spin polarization then precesses on the **z-y** plane around the magnetic field aligned along $\vec{x}$. The precession can be observed as spin quantum beats as the projection of the polarization along $\vec{z}$ changes Fig. 1b. The maxima and minima of the beat signal represent the spin alignments along $\vec{z}$ ($\tau_c = \tau_{max}$) and $-\vec{z}$ ($\tau_c = \tau_{min}$), respectively, while zero represents alignment along $\vec{y}$ ($\tau_c = \tau_0$). A control pulse, to all orders, rotates the spin polarization around $\vec{z}$ an angle equal to the pulse area θ_c of the control pulse. A special case of the rotation is when the spin polarization is along $\vec{y}$ and the control pulse area is set to be $\pi/2$. This rotation puts the spin polarization along $\vec{x}$, which has no precessing components because it is in the eigenstate of the charged QD system under a Voigt magnetic field. This rotation serves a very similar purpose to spin state initialization. In Fig. 1d, we can clearly see the beat amplitudes at $\tau_c = \tau_0$ diminish to almost zero, representing nearly complete alignment in $\vec{x}$. At $\tau_c = \tau_{min}(\tau_{max})$, the beat amplitude is nearly unaffected, representing complete
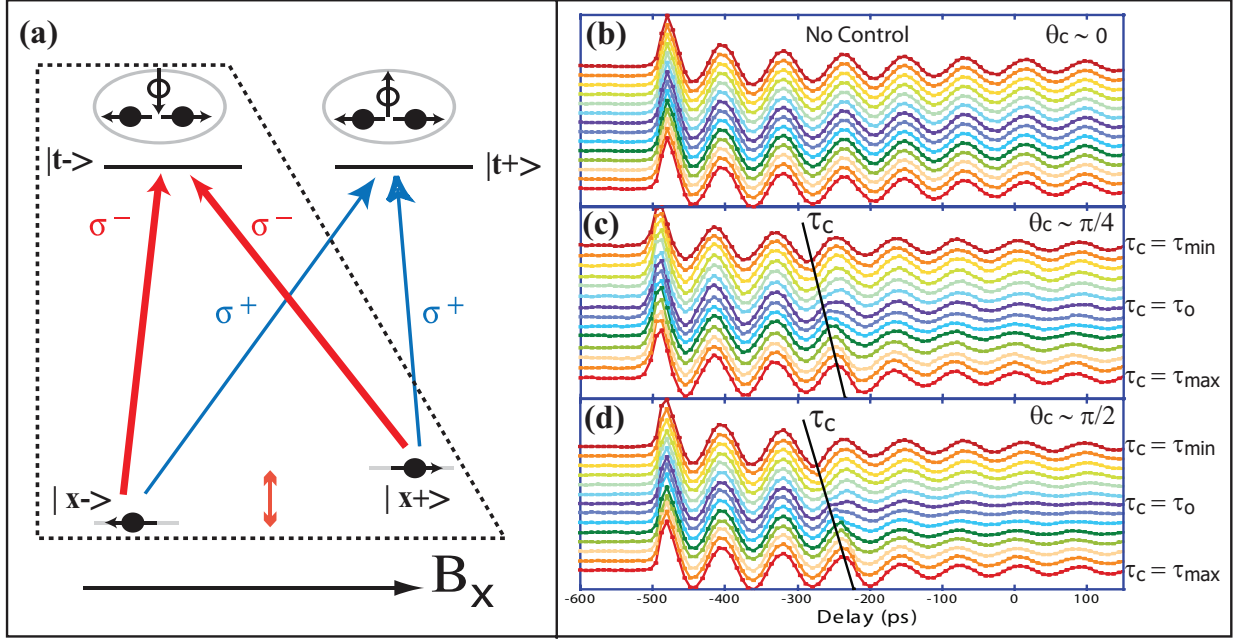
Fig. 1. (a). Energy level diagram in a single charged QD. $|x\pm\rangle$ are the spin ground states and $|t\pm\rangle$ are the trion states. A Λ system can be isolated by using σ_- polarized light as seen in the dashed box. (b) to (d) Three-beam spin quantum beats with pump-probe pair and a control beam, where the control beam delay τ_c is varied from τ_{min} to τ_{max}. θ_c is the control pulse area, where $\theta_c = 0$ in (b), $\theta_c = \pi/4$ in (c), and $\theta_c = \pi/2$ in (d).

alignment in $\vec{z}(-\vec{z})$.

By observing the spin amplitude change at $\tau_c = \tau_0$ for three different $\theta_c = 0, \pi/4, \pi/2$ Fig. 1b-d, we note that the extend of the spin rotation depends on the control pulse area. This behavior is analogous to the Rabi oscillations of a two-level system. It is predicted by theory that by increasing θ_c beyond $\pi/2$ [6], the beats will be revived because the rotation overshoots $\vec{x}$ and the spin gains a $\vec{y}$ component which does precess around the magnetic field. However, this effect is hindered by inhomogeneous broadening and scattering making it difficult to realize in an ensemble.

Our current efforts aim towards performing the same measurements on single charged QDs, which should show more pronounced prove of the realization of spin initialization and spin Rabi oscillations.

References

1. M. Kroutvar et al., "Optically programmable electron spin memory using semiconductor quantum dots", *Nature* **432**, 81 (2004).
2. J. M. Elzerman et al., "Single-shot read-out of an individual electron spin in a quantum dot" *Nature* **430**, 431 (2004).
3. R. Hanson et al., "Single-shot read-out of electron spin states in a quantum dot using spin-dependent tunnel rates", *Phys. Rev. Lett.* **94**, 196802 (2005).
4. J. R. Petta et al., "Coherent Manipulation of Coupled Electron Spins in Semiconductor Quantum Dots", *Science* **309**, 2180 (2005).
5. C. Piermarocchi et al., "Optical RKKY Interaction between Charged Semiconductor Quantum Dots", *Phys. Rev. Lett.* **89**, 167402 (2002).
6. Notes prepared by collaborators, L. Sham and S. Economou.